EBioMedicine xxx (2017) xxx–xxx

Contents lists available at ScienceDirect

EBioMedicine

journal homepage: www.ebiomedicine.com

Research Paper

Deficiency of PTP1B Attenuates Hypothalamic Inflammation via Activation of the JAK2-STAT3 Pathway in Microglia

Taku Tsunekawa [a], Ryoichi Banno [a,*], Akira Mizoguchi [a], Mariko Sugiyama [a], Takashi Tominaga [a], Takeshi Onoue [a], Daisuke Hagiwara [a], Yoshihiro Ito [a], Shintaro Iwama [a,b], Motomitsu Goto [a], Hidetaka Suga [a], Yoshihisa Sugimura [a], Hiroshi Arima [a]

[a] Department of Endocrinology and Diabetes, Nagoya University Graduate School of Medicine, 65 Tsurumai-cho, Showa-ku, Nagoya 466-8550, Japan
[b] Research Center of Health, Physical Fitness and Sports, Nagoya University, Nagoya 464-8601, Japan

ARTICLE INFO

Article history:
Received 4 October 2016
Received in revised form 5 January 2017
Accepted 5 January 2017
Available online xxxx

Keywords:
Protein tyrosine phosphatase-1B
Hypothalamic inflammation
High fat diet
Microglia
Obesity
Signal transducer and activator of transcription-3

ABSTRACT

Protein tyrosine phosphatase 1B (PTP1B) regulates leptin signaling in hypothalamic neurons via the JAK2-STAT3 pathway. PTP1B has also been implicated in the regulation of inflammation in the periphery. However, the role of PTP1B in hypothalamic inflammation, which is induced by a high-fat diet (HFD), remains to be elucidated. Here, we showed that STAT3 phosphorylation (p-STAT3) was increased in microglia in the hypothalamic arcuate nucleus of PTP1B knock-out mice (KO) on a HFD, accompanied by decreased *Tnf* and increased *Il10* mRNA expression in the hypothalamus compared to wild-type mice (WT). In hypothalamic organotypic cultures, incubation with TNFα led to increased p-STAT3, accompanied by decreased *Tnf* and increased *Il10* mRNA expression, in KO compared to WT. Incubation with p-STAT3 inhibitors or microglial depletion eliminated the differences in inflammation between genotypes. These data indicate an important role of JAK2-STAT3 signaling negatively regulated by PTP1B in microglia, which attenuates hypothalamic inflammation under HFD conditions.

1. Introduction

Obesity is a typical lifestyle-related disease (Stein and Colditz, 2004). The disrupted balance between energy intake and energy expenditure causes obesity, which is defined as the excess accumulation of fat mass (Friedman, 2009). Diet-induced obesity is associated with inflammation not only in the peripheral tissues but also in the hypothalamus (De Souza et al., 2005), by which energy balance is primarily regulated (Morton et al., 2006). The consumption of a high-fat diet (HFD) increases the expression levels of tumor necrosis factor-alpha (TNFα) and interleukin-6 (IL-6) in the arcuate nucleus and lateral hypothalamus (Thaler et al., 2012; De Souza et al., 2005), leading to leptin resistance (De Souza et al., 2005; Zhang et al., 2008; De Git and Adan, 2015). The hypothalamic inflammation induced by a HFD is reported to occur prior to substantial body weight gain, suggesting that it might play a causal role in obesity (Valdearcos et al., 2014; Thaler et al., 2012; De Git and Adan, 2015). Recent studies suggest that glial cells, including microglia, are involved in the inflammatory processes in response to a HFD (De Git and Adan, 2015; Argente-Arizon et al., 2015), although the precise mechanisms by which glial cells regulate hypothalamic inflammation remain to be elucidated.

Protein tyrosine phosphatase 1B (PTP1B) is a non-receptor tyrosine phosphatase that is widely expressed in the body, and negatively regulates leptin signaling by dephosphorylating Janus Activating Kinase 2 (JAK2) in the hypothalamus (Tsou and Bence, 2012; Myers et al., 2001; Zhang et al., 2015). Animals under HFD conditions show increased PTP1B expression in the hypothalamus (Zabolotny et al., 2008), and that increase facilitates the storage of body fat (Picardi et al., 2008; White et al., 2009; Zabolotny et al., 2008). Moreover, PTP1B–deficiency in the whole body, brain or proopiomelanocortin (POMC) neurons leads to the increased phosphorylation of JAK2, and protects against obesity induced by a HFD (Klaman et al., 2000; Bence et al., 2006; Banno et al., 2010; Zabolotny et al., 2002; Cheng et al., 2002). PTP1B has also been implicated in the regulation of inflammatory responses in cells, including

* Corresponding author.
E-mail addresses: tsune-ta@med.nagoya-u.ac.jp (T. Tsunekawa), ryouichi@med.nagoya-u.ac.jp (R. Banno), mizoguchi.akira@med.nagoya-u.ac.jp (A. Mizoguchi), sugiyama.mariko@med.nagoya-u.ac.jp (M. Sugiyama), t999tommy@med.nagoya-u.ac.jp (T. Tominaga), t-onoue@med.nagoya-u.ac.jp (T. Onoue), d-hagiwara@med.nagoya-u.ac.jp (D. Hagiwara), yoshi716@med.nagoya-u.ac.jp (Y. Ito), siwama@med.nagoya-u.ac.jp (S. Iwama), goto@med.nagoya-u.ac.jp (M. Goto), sugahide@med.nagoya-u.ac.jp (H. Suga), sugiyosi@med.nagoya-u.ac.jp (Y. Sugimura), arima105@med.nagoya-u.ac.jp (H. Arima).

http://dx.doi.org/10.1016/j.ebiom.2017.01.007

macrophages, myeloid cells and microglia (Zhang et al., 2013; Grant et al., 2014; Pike et al., 2014; Song et al., 2016). However, the role of PTP1B in hypothalamic inflammation induced by a HFD has yet to be clarified.

In the present study, we employed PTP1B KO mice and investigated the role of PTP1B in hypothalamic inflammation induced by a HFD.

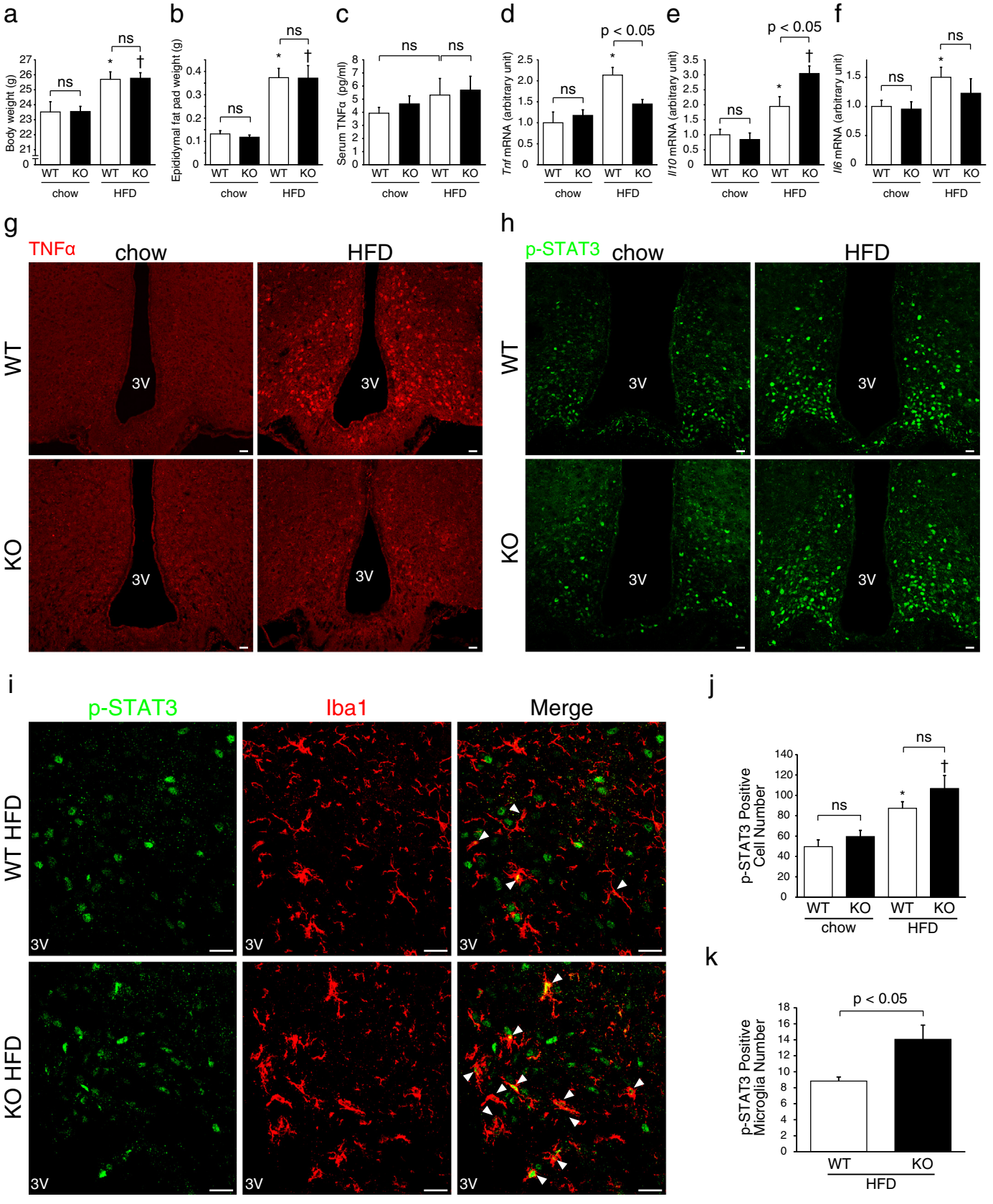

Please cite this article as: Tsunekawa, T., et al., Deficiency of PTP1B Attenuates Hypothalamic Inflammation via Activation of the JAK2-STAT3 Pathway in Microglia, EBioMedicine (2017), http://dx.doi.org/10.1016/j.ebiom.2017.01.007

2. Materials and Methods

2.1. Animals

PTP1B$^{-/-}$ mice (Klaman et al., 2000; Zabolotny et al., 2002) were produced by intercrossing male and female heterozygotes; their PTP1B$^{+/+}$ littermates were used as control mice. All animal procedures were approved by the Animal Care and Use Committee of Nagoya University Graduate School of Medicine and performed in accordance with the institutional guidelines that conform to the National Institutes of Health animal care guidelines. Mice were maintained on a 12 h light/12 h dark cycle in a temperature-controlled barrier facility, with free access to water and food. Age-matched littermates were used for all experiments.

2.2. Food and body composition

At weaning (3 weeks old), male mice were placed on diets of either a standard chow (CE-2, CLEA Japan, Tokyo, Japan; 24.9% protein, 4.6% fat and 70.5% carbohydrate) or a custom high fat diet (Test Diet 58Y1, PMI Nutrition International, KS, USA; 18.3% protein, 60.9% fat, and 20.1% carbohydrate). The composition of fats in the high fat diet was as follows: 39.2% total saturated fatty acids, 40.1% total monounsaturated fatty acids, 13.5% linoleic acid, 1.1% linolenic acid, 0.2% arachidonic acid and 1.1% omega-3 fatty acids. Body weight was monitored until the age of 16 weeks.

2.3. Measurement of Epididymal Fat Pad Weight and Serum TNFα Levels

Measurement of epididymal fat pad weight and collection of blood for measuring serum TNFα levels from mice were performed at the age of 7 weeks in the beginning of the light cycle (between 09:00 and 10:00 a.m.) when mice were in the fed state. Blood was collected via submandibular bleeding. Serum was separated by centrifugation at 9000 rpm, and the serum levels of TNFα were measured by ELISA (Affymetrix eBioscience, CA, USA).

2.4. Extraction of Arcuate Nucleus

Mice were sacrificed in the light cycle between 09:00 and 10:00 a.m., and the arcuate nucleus of the hypothalamus was rapidly dissected from 1.0-mm thick sagittal sections of fresh brain. The arcuate nucleus, the ventral part of the medial hypothalamus with anterior and dorsal margins (approximately 0.5 mm from the ventral surface of the medial hypothalamus) and posterior margin (border with the mammillary body), was dissected using an Alto Stainless Steel Sagittal 1.0 mm Brain Matrix (Roboz Surgical Instrument Co., MD, USA) and Sharp Matrix Blades (Kent Scientific Co., CT, USA) (Minokoshi et al., 2004). The dissected arcuate nucleus was immediately frozen in liquid nitrogen until RNA extraction.

2.5. Brain Collection for Immunohistochemistry

Mice were deeply anesthetized and transcardially perfused with a cold fixative containing 4% paraformaldehyde (PFA) in phosphate buffered saline (PBS) pH 7.4, between 09:00 and 10:00 a.m. in the fed state. After fixation, brains were removed and immersed in the same fixative for 2 h at 4 °C. The brains were kept in PBS containing 10–20% sucrose at 4 °C for cryoprotection. They were embedded in Tissue-Tek O.C.T. compound (Sakura Finetek, Tokyo, Japan) and stored at −80 °C until sectioning. Brains were cut into 20-μm sections on a cryostat at −20 °C, thawed and mounted on Superfrost Plus microscope slides (Matsunami, Tokyo, Japan), and stored at −80 °C until immunohistochemistry was performed as described previously (Ito et al., 2013).

2.6. Intracerebroventricular Injection of TNFα

After 12 h fasting, male WT and KO mice at the age of 10 weeks on a chow diet were deeply anesthetized and placed into a small animal stereotaxic instrument (KOPF, CA, USA). Mice were implanted with a Hamilton needle (2.0 μL syringe) into the right lateral ventricle of the brain (0.34 mm posterior to bregma, 1.0 mm lateral to the midline, and 2.6 mm below the surface of the skull). TNFα (10^{-12} M) or saline in a volume of 2.0 μL was injected into the lateral ventricle over 1 min. Fifteen min after injection, mice were transcardially perfused with a cold fixative containing 4% PFA in sterile PBS pH 7.4, and analyzed with immunohistochemistry. The correct position of the intracerebroventricular (icv) injection was confirmed under the microscope with Hamilton needle marks recognized on the 20 μm brain sections cutting by cryostat.

2.7. Intraperitoneal Injection of Leptin

In order to compare the signaling between TNFα and leptin, 10-week-old mice on a chow diet were employed for ip injection of leptin as well. Male WT and KO mice were fasted overnight (12 h) and injected intraperitoneal (ip) with mouse recombinant leptin (A.F. Parlow, National Hormone and Peptide Program [NHPP], Harbor–UCLA Medical Center, Torrance, California; 1 μg/g body weight) as described previously (Banno et al., 2010; Shibata et al., 2016). Forty-five min after injection, mice were anesthetized and perfused with 4% PFA in PBS, pH 7.4.

2.8. Hypothalamic organotypic cultures

Sixteen-day-old WT and KO mice were sacrificed by decapitation, and hypothalamic tissues were sectioned at 350 μm thicknesses on a Mcllwain tissue chopper (Mickle Laboratory Engineering Co., Surrey, UK). Four coronal slices containing the arcuate nucleus were separated and placed in HBSS (Invitrogen, Grand Island, NY, USA) enriched with glucose. Explants from individual mice were placed on 0.4 μm Millicell-CM filter inserts (Millipore, Billerica, MA, USA), and each filter insert was placed in a Petri dish (35 mm) containing 1.1 mL of culture medium [75% Earle's MEM, 25% HBSS, 25 U/mL penicillin/streptomycin (Invitrogen, Grand Island, NY, USA), 1 mM L-glutamine, and 5.5 mM glucose]. The culture was maintained for 48 h at 37 °C in 5% CO_2-enriched air under stationary conditions and the medium was changed every 24 h. Incubation with TNFα, STAT3 inhibitors, liposomal clodronate or leptin was performed in each experiment. Total RNA and protein from the hypothalamic slices were extracted 72 h after starting the cultures and subjected to analyses with quantitative real-time PCR (qRT-PCR), Western blot or immunohistochemistry, as described previously (Ito et al., 2012; Adachi et al., 2014; Onoue et al., 2016).

Fig. 1. Hypothalamic inflammation is decreased and p-STAT3-positive microglia are increased in PTP1B KO mice on a HFD. Body weight (a), epididymal fat pad weight (b) and serum TNFα (c) in PTP1B$^{+/+}$ (WT) and PTP1B$^{-/-}$ (KO) mice at the age of 7 weeks on a chow diet or a HFD. (d-f) The mRNA expression levels of *Tnf* (d), *Il10* (e) and *Il6* (f) in the arcuate nucleus of WT and KO male mice at the age of 7 weeks on a chow diet or a HFD ($n = 7$–9). (g) Immunostaining of TNFα in the arcuate nucleus of WT and KO male mice at the age of 7 weeks on a chow diet or a HFD. (h and j) Immunostaining of STAT3 phosphorylation (p-STAT3) (h) and resulting p-STAT3-positive cell numbers (j) in the arcuate nucleus of WT and KO male mice at the age of 7 weeks on a chow diet or a HFD ($n = 4$ for a chow diet; $n = 5$ for a HFD). (i and k) Immunostaining of p-STAT3 and Iba1 in the arcuate nucleus of WT and KO male mice at the age of 7 weeks on a HFD (i), and p-STAT3-positive cell numbers in microglia (k) ($n = 6$). White arrow heads show colocalization of microglia with p-STAT3. All values are means ± SEM. Statistical analyses were performed by either two-way ANOVA (a-f and j) or unpaired *t*-test (k). *, $p < 0.05$ versus chow in WT. †, $p < 0.05$ versus chow in KO. Ns; not significant. Scale bar = 20 μm. 3 V: third ventricle.

Please cite this article as: Tsunekawa, T., et al., Deficiency of PTP1B Attenuates Hypothalamic Inflammation via Activation of the JAK2-STAT3 Pathway in Microglia, EBioMedicine (2017), http://dx.doi.org/10.1016/j.ebiom.2017.01.007

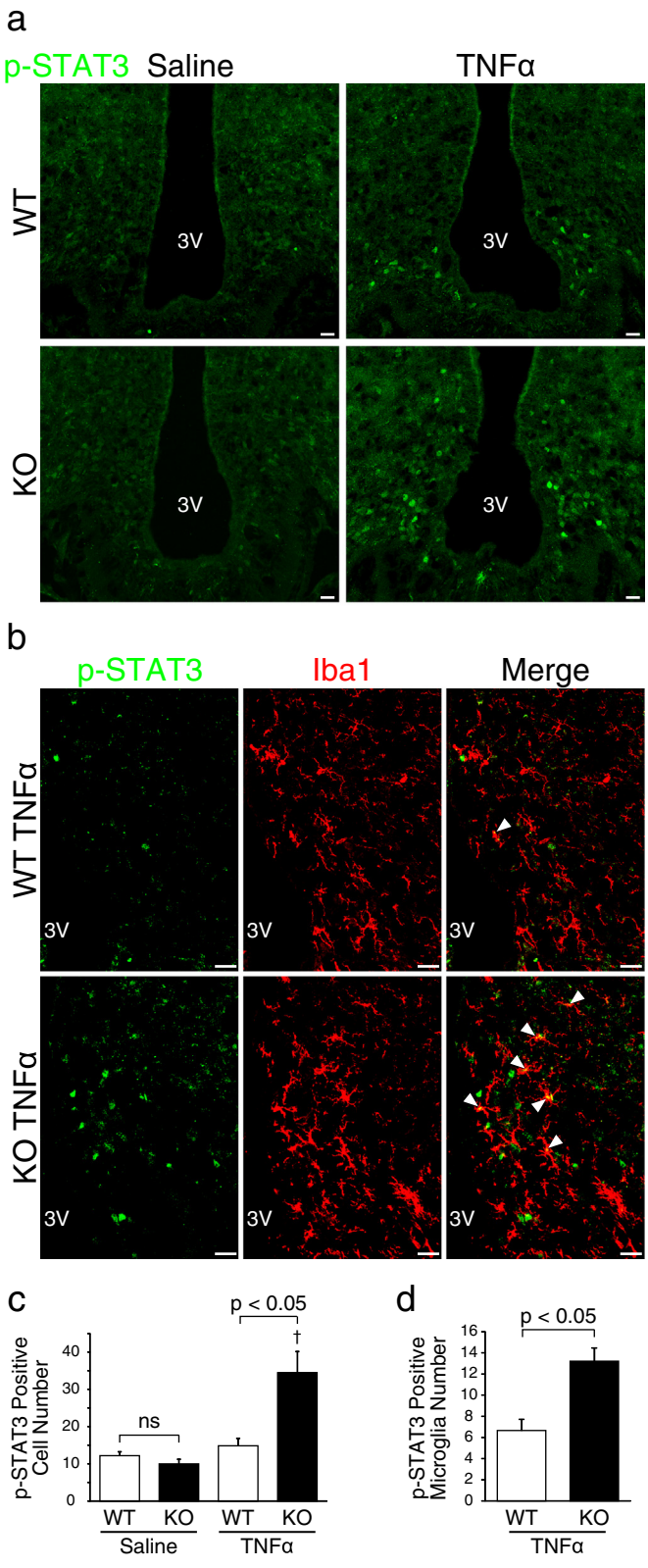

Fig. 2. TNFα induces the phosphorylation of STAT3 in microglia but not in astrocytes or neurons in the hypothalamus in KO mice. (a and c) Immunostaining of p-STAT3 (a) and p-STAT3-positive cell numbers (c) in the arcuate nucleus after icv injection of saline or 10^{-12} M TNFα into WT and KO male mice at the age of 10 weeks on a chow diet after 12 h fasting ($n = 4$ for saline; $n = 5$ for TNFα). (b and d) Immunostaining of p-STAT3 and Iba1 (b) in the arcuate nucleus after icv injection of 10^{-12} M TNFα, and p-STAT3-positive cell numbers in microglia (d) ($n = 5$). White arrow heads show colocalization of microglia with p-STAT3. All values are means ± SEM. Statistical analyses were performed by either two-way ANOVA (c) or unpaired *t*-test (d). †, $p < 0.05$ versus saline in KO. Ns; not significant. Scale bar = 20 μm, 3 V; third ventricle.

2.9. Effects of TNFα on the mRNA Expression and the Phosphorylation of Signal-transducing Proteins Downstream of TNFα Receptor Signaling in Hypothalamic Slice Cultures

To examine the time-course of TNFα effects on mRNA expression levels of *Ptpn1* and inflammatory cytokines (*Tnf*, *Il10*, *Il6* and *Il1b*), hypothalamic slice cultures were incubated with 100 ng/mL TNFα (R&D systems, MN, USA) for 0.5, 1, 2, 3, 6 or 24 h, while control explants were incubated with a vehicle (sterile PBS) for 0.5 h, and total RNA and proteins were extracted. To examine the dose-response of TNFα on inflammatory cytokines, hypothalamic explants were incubated with vehicle or TNFα (25, 50 or 100 ng/mL) for 1 h. For the dose-response of TNFα on *Ptpn1*, hypothalamic explants were incubated for 3 h. To examine the effects of TNFα on phosphorylation of JAK2, STAT3, mitogen-activated protein kinase (MAPK) and NFκB p65, hypothalamic explants were incubated with TNFα (100 ng/mL) for 0.5 h, and total RNA and protein were extracted.

2.10. Effects of STAT3 Inhibitor on TNFα-induced Cytokine Expression in Hypothalamic Slice Cultures

In order to determine whether PTP1B-mediation of the expression of inflammatory cytokines occurred through the JAK2-STAT3 pathway, hypothalamic slices were incubated with two classes of STAT3 inhibitor, JSI-124 (0.5 or 5 μM; Sigma-Aldrich, MO, USA) for 4 h or S31-201 (30 or 100 μM; Santa Cruz Biotechnology, TX, USA) for 2 h. Dimethyl sulfoxide (DMSO, Wako, Osaka, Japan) was used as the control. The slices were incubated with TNFα (100 ng/mL) or vehicle (sterile PBS) together with JSI-124, S31-201 or DMSO for an additional 0.5 h, and total RNA and protein were extracted.

2.11. Depleting Microglia from Hypothalamic Slice Cultures

After establishing the cultures (24 h), we incubated the hypothalamic slices with 1.0 mg/mL of liposomal clodronate (Clo), which reportedly depleted microglial cells without altering other cell types (Vinet et al., 2012; Valdearcos et al., 2014), or with control liposomes (Lip) (Cosmobio, Tokyo, Japan) for 24 h. Slices were then placed in fresh medium, and 24 h later slices were treated with TNFα (100 ng/mL) or vehicle (sterile PBS) for 0.5 h, and total RNA and protein were extracted. For the evaluation of Iba1, GFAP and NeuN expression in hypothalamic slice cultures, the slices were fixed with 4% formaldehyde in PBS for 30 min, washed twice in PBS and kept in PBS containing 10–20% sucrose at 4 °C for cryoprotection. They were embedded in Tissue-Tek O.C.T. compound (Sakura Finetek, Tokyo, Japan) and stored at −80 °C until sectioning. Slices were cut into 30-μm sections on a cryostat at −20 °C, thaw mounted on Superfrost Plus microscope slides (Matsunami, Tokyo, Japan), stored at −80 °C and analyzed with immunohistochemistry as described previously (Hagiwara et al., 2014; Sato et al., 2005).

2.12. Effects of Leptin on Cytokine and Ptpn1 Expression in Hypothalamic Slice Cultures

Hypothalamic slices were incubated in the absence or presence of 100 ng/mL TNFα and 10^{-7} M leptin for 0.5 h, and total RNA and protein were extracted. To examine the effects of leptin on *Ptpn1* mRNA expression, hypothalamic explants were incubated with leptin (10^{-8} M, 10^{-7} M or 10^{-6} M) or PBS (vehicle) for 24 h.

2.13. Determination of mRNA Levels by qRT-PCR

Total RNA was extracted from samples using TRIzol (Invitrogen, CA, USA) and the RNeasy kit (QIAGEN, Hilden, Germany). cDNA was synthesized from 100 ng total RNA using ReverTra Ace qPCR RT Kit (TOYOBO, Osaka, Japan). The qRT-PCR reactions were carried out

Please cite this article as: Tsunekawa, T., et al., Deficiency of PTP1B Attenuates Hypothalamic Inflammation via Activation of the JAK2-STAT3 Pathway in Microglia, EBioMedicine (2017), http://dx.doi.org/10.1016/j.ebiom.2017.01.007

using Brilliant III Ultra-Fast SYBR Green QPCR Master Mix (Agilent Technologies, CA, USA), and samples were run using the Stratagene Mx3000p. The relative mRNA levels of *Tnf*, *Il10*, *Il1b*, *Il6*, *Ptpn1*, *Iba1*, *Cd68*, *Adgre1*, *Gfap*, *Tubb3*, *Pomc* and *Agrp* in the arcuate nucleus or the hypothalamus slice explants were assessed by qRT-PCR using *Gapdh* as an internal control. The qRT-PCR reactions were carried out, and relative mRNA expression levels were calculated using the comparative Ct method as described previously (Ito et al., 2013). The sequences of primers are described in Supplementary Table 1.

2.14. Determination of Protein Levels by Western Blot

Samples of hypothalamic slices were lysed in 100 μL of a buffer containing 10 mM Tris (pH 7.4), 50 mM NaF, 150 mM NaCl, 0.1% SDS, 2 mM Na_3VO_4, 5 mM EDTA, 1% Triton X-100 (Sigma-Aldrich, MO, USA) 1% sodium deoxycholate minimum and 1% protease inhibitor mix (Roche, Stockholm, Sweden). After centrifuging the samples, protein concentrations in the supernatants were determined using a bicinchoninic acid kit (Sigma-Aldrich, MO, USA). Protein (5–10 μg per sample) was run on a 10% Bis–Tris gel (Invitrogen) and transferred onto PVDF membranes (Millipore, MA, USA). Blots were blocked for 1 h in TBS-T solution [10 mM Tris–HCl (pH 7.4), 150 mM NaCl, and 0.1% Tween] containing 5% skim milk or 5% bovine serum albumin (Wako, Osaka, Japan). Membranes were incubated with antibodies against STAT3 phosphorylated at Tyr705, phospho-ERK, phospho-JNK, phospho-p38MAPK or phospho-NFκB p65 (Cell Signaling, MA, USA) or phospho-JAK2 (Invitrogen) overnight at 4 °C. Primary antibodies were probed with HRP-conjugated donkey anti-rabbit IgG (NA934; GE Healthcare, Little Chalfont, UK) for 1 h at room temperature. To improve sensitivity and signal-to-noise ratio, Can Get Signal Immunoreaction Enhancer Solution (TOYOBO, Osaka, Japan) was used for the dilution of the primary and secondary antibodies. Immunoreactivity was detected using the ECL Prime Western Blotting Detection Reagent (GE Healthcare). The membranes were stripped and incubated with antibodies against each nonphosphorylated protein or β-actin antibody (Abcam, Cambridge, UK) for normalization.

2.15. Immunohistochemistry

For detection of TNFα, the frozen sections were washed with PBS, 0.3% Triton X-100 in PBS (15 min) and 50 mM glycine (15 min) followed by blocking with a mixture of 3% bovine serum albumin (Wako, Osaka, Japan) in PBS for 1 h at room temperature. Next, the sections were incubated with anti-TNFα antibody (1:50; R&D systems, MN, USA) overnight at 4 °C. The sections were then treated with Alexa Fluor 594-conjugated anti-goat IgG secondary antibody (1:500; Invitrogen) for 1 h at room temperature. After washing in 1 × PBS, sections were placed on slides, air dried, and cover slipped with Vectashield (Vector Labs, CA, USA).

Immunohistochemistry of STAT3 phosphorylation was performed as described previously (Banno et al., 2010). Sections were washed with 1× PBS prior to and between successive blocking steps with 1.0% H_2O_2 / 1.0% NaOH in H_2O (20 min), 0.3% glycine (10 min), 0.03% SDS (10 min) and finally 0.2% sodium azide/ 3% normal goat serum / 0.25% Triton X-100 in PBS (1 h) at room temperature. Sections were then incubated with anti-p-STAT3 antibody (1:100; Cell Signaling, MA, USA), anti-Iba1 (1:100, Wako, Osaka, Japan), anti-GFAP (1:100; Sigma-Aldrich, MO, USA) or anti-NeuN (1:100; Merck Millipore, Darmstadt, Germany) and then diluted in azide blocking solution overnight at 4 °C. The following day, sections were washed with 1× PBS and subsequently in sodium azide–free blocking solution containing Alexa Fluor 488-conjugated anti-rabbit IgG secondary antibody (1:500; Invitrogen), Alexa Fluor 594-conjugated anti-mouse IgG secondary antibody (1:500; Invitrogen) or Alexa Fluor 647-conjugated anti-chicken IgY secondary antibody (1:500; Invitrogen) for 1 h at room temperature. After

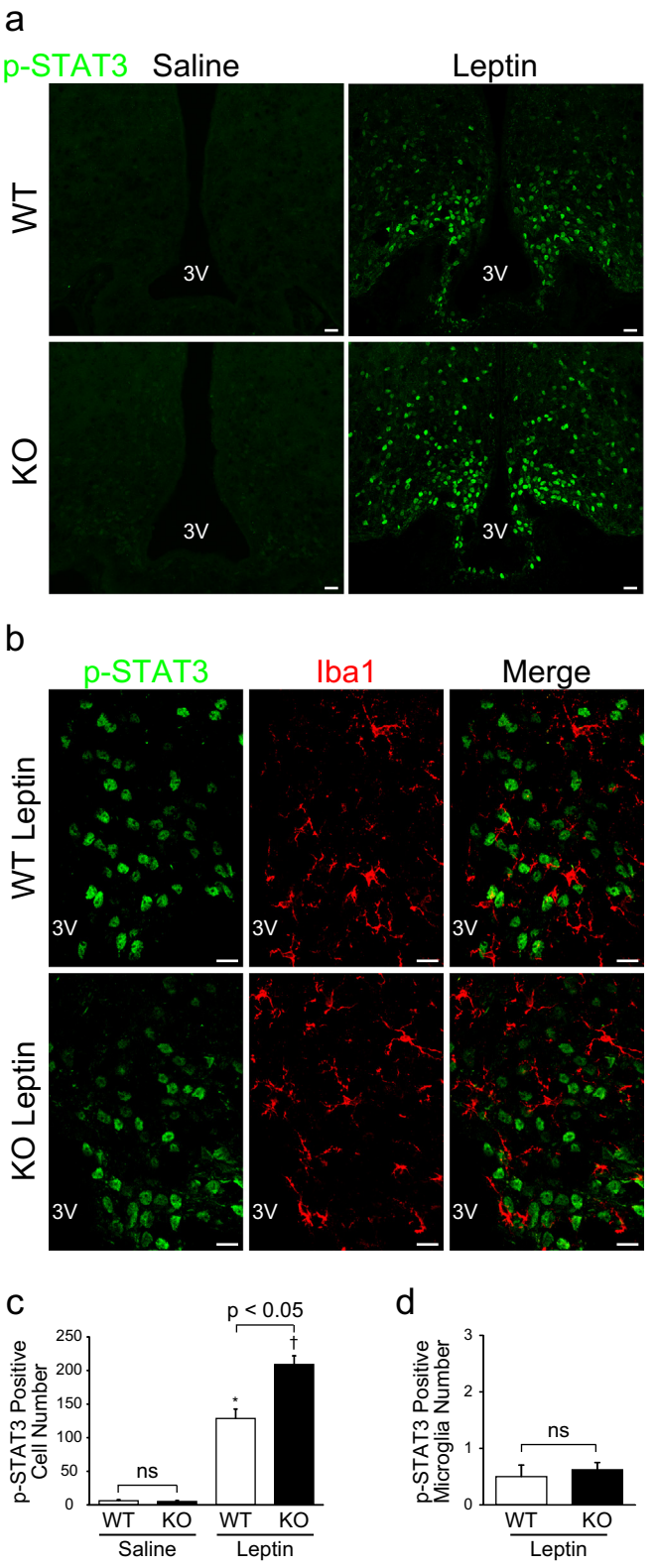

Fig. 3. Leptin induces STAT3 phosphorylation in astrocytes and neurons but not in microglia in the hypothalamus. (a and c) Immunostaining of p-STAT3 cells (a) and the p-STAT3-positive cell numbers (c) in the arcuate nucleus after ip injection of saline or 1 μg/g leptin in WT and KO male mice at the age of 10 weeks on a chow diet after 12 h fasting ($n = 4$). (b and d) Immunostaining of p-STAT3 and Iba1 (b) in the arcuate nucleus after ip injection of saline or 1 μg/g leptin, and the p-STAT3-positive cell numbers in microglia (d) ($n = 4$). All values are means ± SEM. Statistical analyses were performed by either two-way ANOVA (c) or unpaired *t*-test (d). *, $p < 0.05$ versus saline in WT. †, $p < 0.05$ versus saline in KO. Ns; not significant. Scale bar = 20 μm. 3 V: third ventricle.

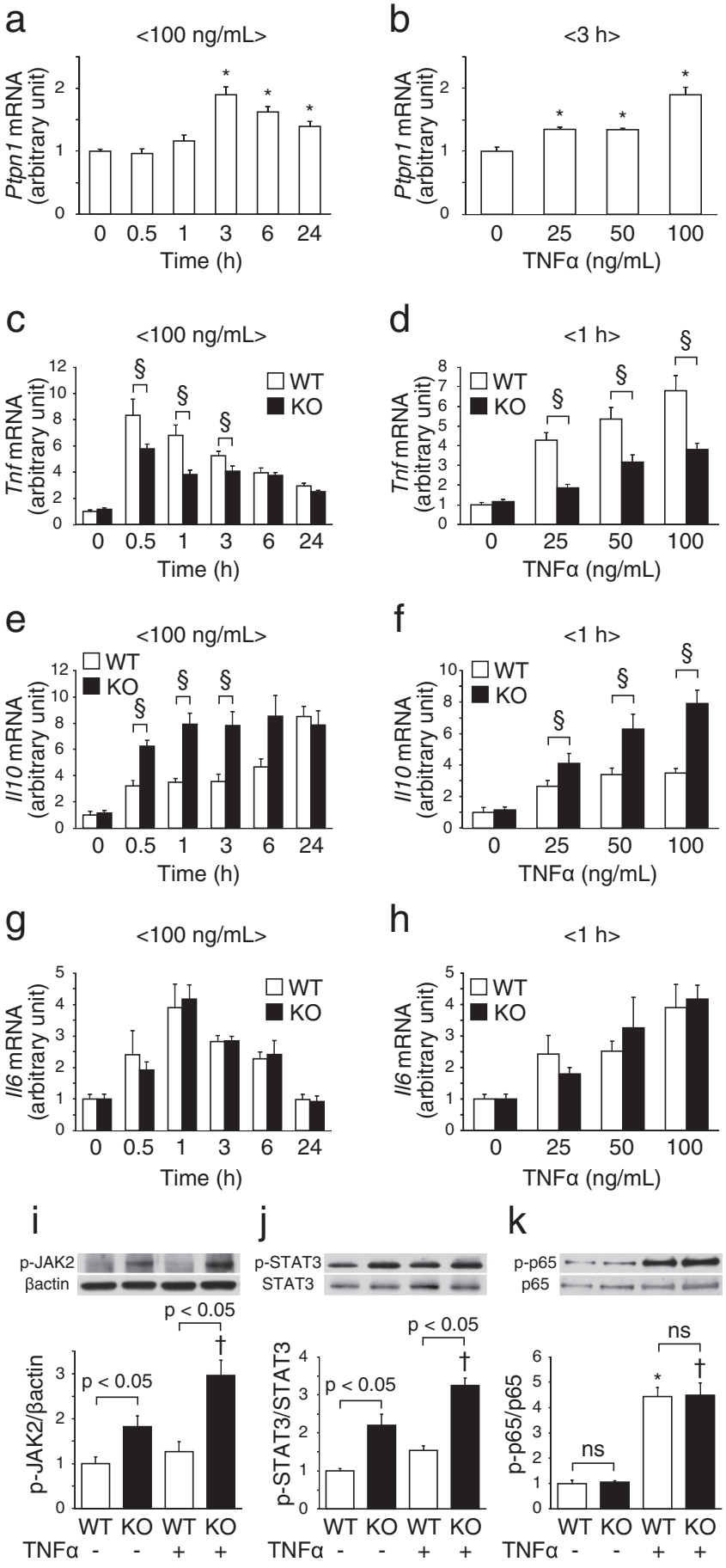

Please cite this article as: Tsunekawa, T., et al., Deficiency of PTP1B Attenuates Hypothalamic Inflammation via Activation of the JAK2-STAT3 Pathway in Microglia, EBioMedicine (2017), http://dx.doi.org/10.1016/j.ebiom.2017.01.007

washing in 1× PBS, sections were placed on slides, air dried, and cover slipped with Vectashield (Vector Labs).

Immunohistochemistry of PTP1B was performed as described previously (Dodd et al., 2015). Sections were subjected to antigen retrieval in citrate acid buffer [10 mM sodium citrate, 0.05% (v/v) Tween 20, pH 6.0] at 85 °C for 20 min. Sections were incubated at room temperature for 1 h in blocking buffer [0.1 M phosphate buffer, 0.2% (v/v) Triton X-100, 10% (v/v) bovine serum albumin (Wako, Osaka, Japan)] and then overnight at 4 °C with anti-PTP1B antibody (1:200; R&D systems, MN, USA), anti-Iba1 antibody(1:100; Wako Osaka, Japan), anti-GFAP (1:100; Sigma-Aldrich, MO, USA) or anti-NeuN antibody (1:200; Merck Millipore, Darmstadt, Germany) in blocking buffer. After washing with PBS, sections were incubated with Alexa Fluor 488-conjugated anti-goat IgG secondary antibody (1:500; Invitrogen), Alexa Fluor 594-conjugated anti-rabbit IgG secondary antibody (1:500; Invitrogen), Alexa Fluor 594-conjugated anti-mouse IgG secondary antibody (1:500; Invitrogen) or DyLight 650-conjugated anti-chicken IgY secondary antibody (1:500; Abcam, Cambridge, UK) in blocking buffer for 2 h at room temperature. After washing in 1× PBS, sections were placed on slides, air dried, and cover slipped with Vectashield (Vector Labs).

All fluorescently stained sections were examined with a confocal laser microscope (TiEA1R; NIKON INSTECH, Tokyo, Japan) and viewed using NIS-Elements software (NIKON INSTECH, Tokyo, Japan). Cells labeled for p-STAT3 were counted bilaterally in a blinded fashion. For analysis, we employed 4–6 mice in each group for the staining, and the mean values of 2 or 3 serial sections from each mouse were calculated. The sections included the arcuate nucleus [−1.70 mm to −1.82 mm from bregma based on coordinates in the brain atlas (Paxinos and Franklin, 2000)]. The sample numbers in figure legends indicate the number of animals analyzed.

2.16. Statistical Analysis

The statistical significance of the differences between groups was analyzed by either unpaired *t*-test, one-way ANOVA, two-way ANOVA or two-way ANOVA with repeated measures followed by Bonferroni's test by using SPSS Statistics 23 (IBM, NY, USA). Results are expressed as means ± SEM, and differences were considered significant at $P < 0.05$.

3. Results

3.1. Hypothalamic Inflammation Induced by HFD is Decreased in PTP1B KO Mice

Both body weight and epididymal fat pad weight of male mice at the age of 7 weeks were significantly higher on a HFD compared to those of mice on a chow diet in both PTP1B$^{+/+}$ (WT) and PTP1B$^{-/-}$ (KO) mice (Fig. 1a, b). While body weights were significantly lower in KO compared to WT mice on a HFD after the age of 8 weeks (Supplementary Fig. 1a), there were no significant differences in body weights and epididymal fat pad weights between genotypes at the age of 7 weeks (Fig. 1a, b). There were no significant differences in serum TNFα levels between mice on a HFD and those on a chow diet, as well as between genotypes (Fig. 1c). On the other hand, tumor necrosis factor (*Tnf*) mRNA expression levels in the arcuate nucleus were significantly increased on a HFD compared with chow in WT, but not in KO mice (Fig. 1d). The analysis of immunofluorescence staining also showed that TNFα immunoreactivity in the arcuate nucleus was increased on a HFD compared with chow in WT, but not in KO mice (Fig. 1g). The interleukin-10 (*Il10*) mRNA expression levels were significantly increased in WT mice on a HFD compared with chow, and the expression levels were further enhanced in KO mice (Fig. 1e). As reported previously (Zabolotny et al., 2008), the mRNA expression levels of the gene for PTP1B (*Ptpn1*) in the arcuate nucleus were significantly increased in WT mice on a HFD compared with chow (Supplementary Fig. 1b). The mRNA expression levels of interleukin-6 (*Il6*) and interleukin-1β (*Il1b)* in the arcuate nucleus were significantly increased on a HFD compared with chow, but there were no significant differences in the expression levels between genotypes (Fig. 1f and Supplementary Fig. 1c).

3.2. PTP1B Immunoreactivity in the Arcuate Nucleus

To examine the localization of PTP1B immunoreactivity in the arcuate nucleus, ionized calcium binding adaptor molecule 1 (Iba1), glial fibrillary acidic protein (GFAP) and neuronal nuclei (NeuN) were used as markers of microglia, astrocytes and neurons, respectively. Double immunostaining revealed that PTP1B-immunoreactivity was observed in the microglia, astrocytes and neurons in WT mice (Supplementary Fig. 1d), whereas no immunoreactivity was observed in KO mice (data not shown).

3.3. HFD Induces the Phosphorylation of STAT3 in Microglia in the Arcuate Nucleus

Signal transducer and activator of transcription 3 (STAT3) phosphorylation in the arcuate nucleus was significantly increased in mice on a HFD compared to chow; there were no significant differences in STAT3 phosphorylation between genotypes (Fig. 1h, j). Double-immunostaining revealed that phospho-STAT3-positive cell numbers were significantly increased in microglia and astrocytes in KO mice compared to WT mice (Fig. 1i, k and Supplementary Fig. 1e, g). In contrast, there were no significant differences in the numbers of phospho-STAT3-positive neurons between genotypes (Supplementary Fig. 1f, h). Similar results were obtained when the percentages of microglia, astrocytes or neurons in pSTAT3-positive cells in the arcuate nucleus were analyzed (Supplementary Table 2).

3.4. TNFα Induces Phospho-STAT3 in Microglia But Not in Astrocytes or Neurons in the Arcuate Nucleus in KO Mice

To evaluate whether TNFα induces hypothalamic STAT3 phosphorylation, we conducted icv injection of 10^{-12} M TNFα. This dose of TNFα did not cause any significant changes in STAT3 phosphorylation in WT mice, whereas STAT3 phosphorylation was significantly increased in the arcuate nucleus in PTP1B KO mice (Fig. 2a, c). The anatomical analysis revealed that phospho-STAT3-positive cell numbers were significantly increased in microglia after TNFα injection in KO compared to WT mice (Fig. 2b, d), whereas there were no significant differences in cell numbers between genotypes in astrocytes and neurons (Supplementary Fig. 2 and Supplementary Table 3).

3.5. Leptin Induces Phospho-STAT3 in Astrocytes and Neurons But Not in Microglia in the Hypothalamus

While ip injection of leptin induced STAT3 phosphorylation in the arcuate nucleus in both WT and KO mice, the phosphorylation was significantly increased in KO mice compared to WT mice (Fig. 3a, c). The phospho-STAT3-positive cell numbers were significantly increased after leptin injection in both astrocytes and neurons in KO compared

Fig. 4. PTP1B–deficiency attenuates inflammation induced by TNFα in hypothalamic cultures. (a and b) Time-course (a) and dose response (b) effects of TNFα on *Ptpn1* mRNA expression in WT mice. (c-h) Time course (c, e and g) and dose response (d, f and h) effects of TNFα on *Tnf* (c and d), *Il10* (e and f) or *Il6* (g and h) mRNA expression in WT and KO mice. (i-k) Effects of 100 ng/mL TNFα on phosphorylation of JAK2 (i), STAT3 (j) and NFκB p65 (k). Levels of each phosphoprotein were normalized to β-actin and STAT3, respectively. All values are means ± SEM ($n = 4$ for control, $n = 6$–8 for TNFα). Statistical analyses were performed by either two-way ANOVA (a and c-k) or one-way ANOVA (b). *, $p < 0.05$ versus control in WT. †, $p < 0.05$ versus control in KO. §, $p < 0.05$ versus TNFα in WT.

Please cite this article as: Tsunekawa, T., et al., Deficiency of PTP1B Attenuates Hypothalamic Inflammation via Activation of the JAK2-STAT3 Pathway in Microglia, EBioMedicine (2017), http://dx.doi.org/10.1016/j.ebiom.2017.01.007

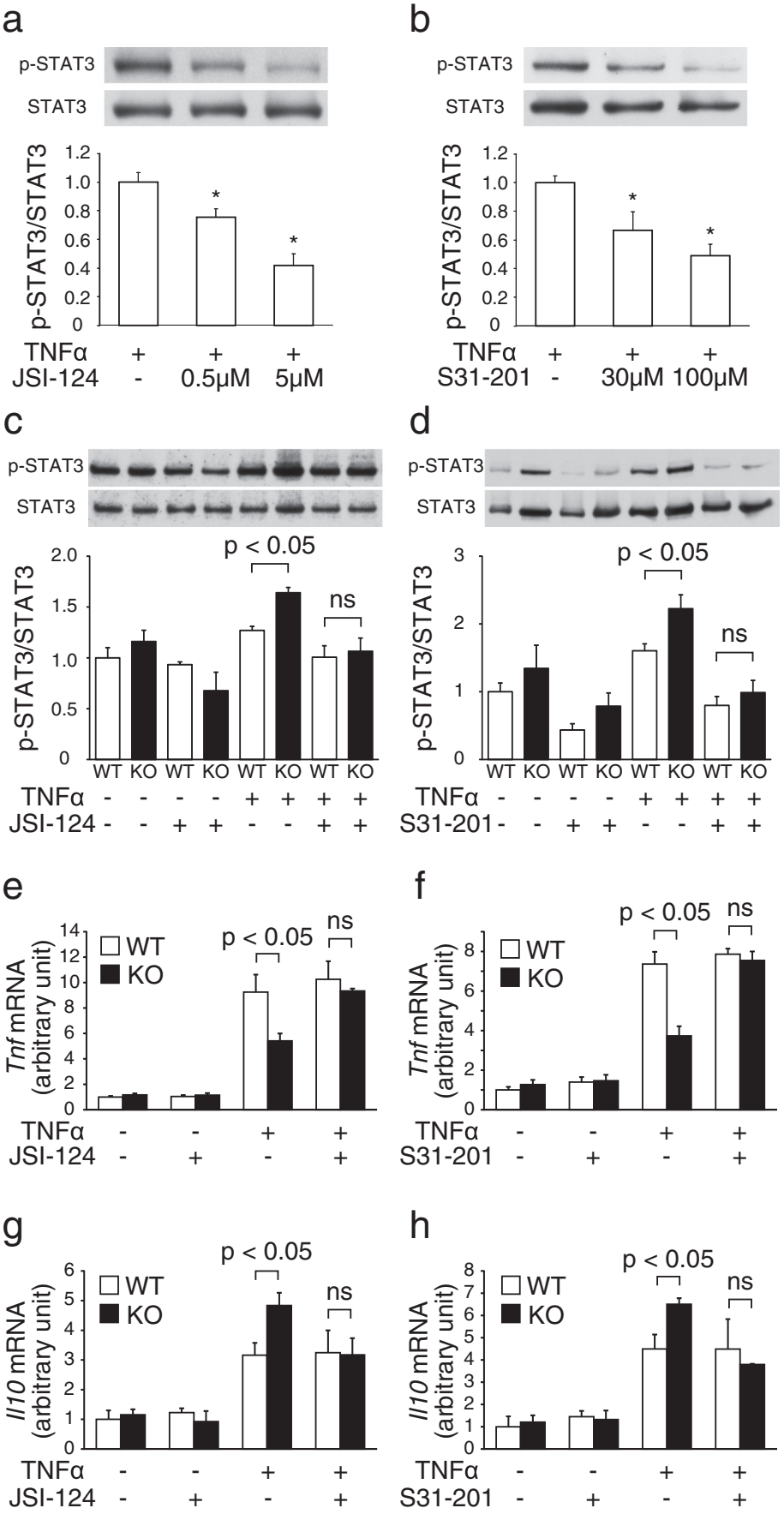

Please cite this article as: Tsunekawa, T., et al., Deficiency of PTP1B Attenuates Hypothalamic Inflammation via Activation of the JAK2-STAT3 Pathway in Microglia, EBioMedicine (2017), http://dx.doi.org/10.1016/j.ebiom.2017.01.007

to WT mice (Supplementary Fig. 3). In contrast, leptin did not induce STAT3 phosphorylation in microglia in WT or KO mice (Fig. 3b, d and Supplementary Table 4).

3.6. PTP1B-deficiency Attenuates Inflammation Induced by TNFα in Hypothalamic Cultures

The incubation of hypothalamic explants with TNFα significantly increased *Ptpn1* mRNA expression levels (Fig. 4a, b). Incubation with TNFα significantly increased *Tnf* and *Il10* mRNA expression levels in both genotypes (Fig. 4c-f). In contrast, the increased *Tnf* mRNA expression levels were significantly attenuated (Fig. 4c, d) and *Il10* mRNA expression levels were significantly increased (Fig. 4e, f) in KO mice compared to WT mice. The increased *Il1b* mRNA expression levels were also significantly attenuated in KO mice compared to WT mice (Supplementary Fig. 4a, b), whereas the *Il6* mRNA expression levels were similar between genotypes (Fig. 4g, h). Incubation with TNFα increased the phosphorylation of both JAK2 and STAT3 in hypothalamic explants in both genotypes. In contrast, phosphorylation was increased to a greater extent in KO mice (Fig. 4i, j). Phosphorylation of other signal-transducing proteins such as p65, p38, c-Jun N-terminal kinase (JNK) and extracellular signal-regulated kinase (ERK) was increased similarly in response to TNFα in both genotypes (Fig. 4k and Supplementary Fig. 4c–e).

3.7. Inhibition of the JAK2-STAT3 Pathway Cancels the Differences of Inflammation Between Genotypes

In order to determine whether the attenuation of hypothalamic inflammation by PTP1B-deficiency was mediated through the JAK2-STAT3 pathway, we treated hypothalamic explants with two classes of STAT3 inhibitors, JSI-124 and S31-201. We confirmed that STAT3 inhibitors decreased STAT3 phosphorylation in a dose-dependent manner (Fig. 5a, b), and that the STAT3 phosphorylation induced by TNFα was decreased to similar levels in both WT and KO mice by the inhibitors (Fig. 5c, d). On the other hand, STAT3 inhibitors did not affect the phosphorylation of other signal-transducing proteins such as p65, p38, JNK and ERK (Supplementary Fig. 5a–d and 5f–i). Incubation with the inhibitors of STAT3 phosphorylation completely inhibited the downregulation of *Tnf* and upregulation of *Il10* mRNA expression in KO mice treated with TNFα (Fig. 5e-h). Incubation with the inhibitors of STAT3 phosphorylation also blocked the downregulation of *Il1b* (Supplementary Fig. 5e, j).

3.8. Microglial Depletion Abolishes the Attenuation of Inflammation by PTP1B-Deficiency

We used liposomal clodronate (Clo) to deplete microglia from the hypothalamic slice cultures; liposomes (Lip) were used as controls. Microglial depletion was confirmed by a marked reduction in the mRNA expression levels of microglial markers such as allograft inflammatory factor 1 (*Aif1*), cluster of differentiation 68 (*Cd68*) and adhesion G protein-coupled receptor E1 (*Adgre1*) (Fig. 6a). In addition, we also confirmed the loss of Iba1-positive cells by immunofluorescence staining (Fig. 6b). Treatment with Clo did not change mRNA expression levels of *Gfap*, tubulin, beta 3 class III (*Tubb3*), *Pomc* or agouti-related protein (*Agrp*) compared to control (Fig. 6a). The expression levels of GFAP or NeuN proteins in immunofluorescently-positively cells were not affected by Clo treatment (Fig. 6b). Microglial depletion remarkably decreased the mRNA expression levels of *Tnf* and

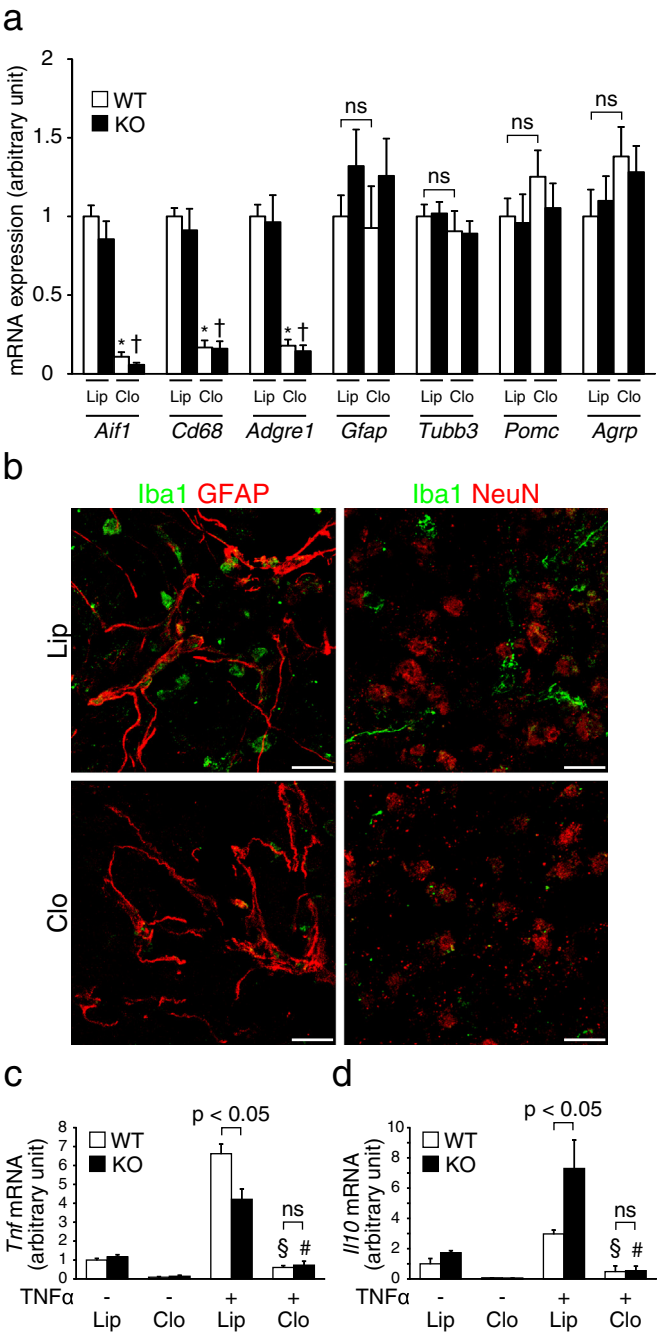

Fig. 6. Microglial depletion abolishes attenuation of inflammation by PTP1B-deficiency. Effect of microglial depletion on gene expression. (a) The mRNA expression levels of *Aif1*, *Cd68*, *Adgre1*, *Gfap*, *Tubb3*, *Pomc* and *Agrp* in cells treated with control liposomes (Lip) or liposomal clodronate (Clo) ($n = 8$). (b) Immunostaining for Iba1 and GFAP or NeuN in cells treated with Lip or Clo. (c and d). Effects of 100 ng/mL TNFα on the mRNA expression level of *Tnf* (c) and *Il10* (d) in cells treated with Lip or Clo ($n = 4$–5). All values are means ± SEM. Statistical analyses were performed by two-way ANOVA. *, $p < 0.05$ versus Lip in WT. †, $p < 0.05$ versus Lip in KO. §, $p < 0.05$ versus Lip and TNFα in WT. #, $p < 0.05$ versus Lip and TNFα in KO. Ns; not significant. Scale bar = 20 μm.

Il10 compared to controls, and completely blocked the downregulation of *Tnf* and upregulation of *Il10* mRNA expression by TNFα in KO mice (Fig. 6c, d).

Fig. 5. Inhibition of the JAK2-STAT3 pathway blocks the suppression of *Tnf* and the induction of *Il10* mRNA expression in KO treated with TNFα. (a, b) Dose response effects of JSI-124 (a) or S31–201 (b) on STAT3 phosphorylation induced by 100 ng/mL TNFα in WT mice. (c, d) STAT3 phosphorylation induced by 100 ng/mL TNFα in the absence or presence of 0.5 μM JSI-124 (c) or 30 μM S31–201 (d) in WT and KO mice ($n = 3$–5). (e–h) Expression of *Tnf* mRNA (e and f) and *Il10* mRNA (g and h) induced by 100 ng/mL TNFα in the absence or presence of 0.5 μM JSI-124 (e and g) or 30 μM S31–201 (f and h) in WT and KO mice ($n = 3$–6). All values are means ± SEM. Statistical analyses were performed by either one-way ANOVA (a and b) or two-way ANOVA (c-h). *, $p < 0.05$ versus TNFα in WT. Ns; not significant.

Please cite this article as: Tsunekawa, T., et al., Deficiency of PTP1B Attenuates Hypothalamic Inflammation via Activation of the JAK2-STAT3 Pathway in Microglia, EBioMedicine (2017), http://dx.doi.org/10.1016/j.ebiom.2017.01.007

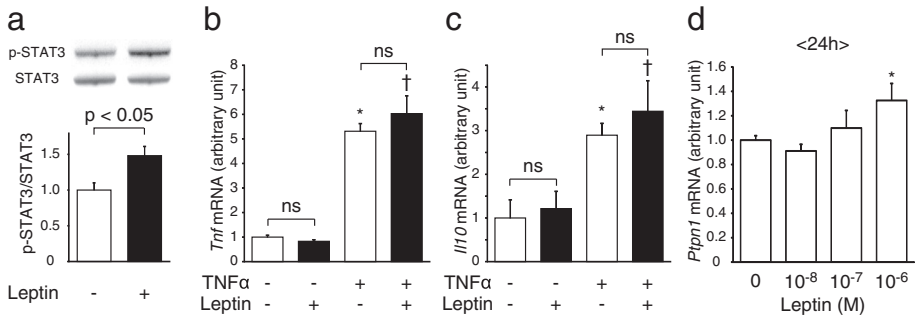

Fig. 7. STAT3 phosphorylation induced by leptin does not affect hypothalamic inflammation induced by TNFα. (a–c) STAT3 phosphorylation in cells (a) treated with 10^{-7} M leptin in hypothalamic slice explants of WT mice, and expression of *Tnf* mRNA (b) and *Il10* mRNA (c) induced by 100 ng/mL TNFα treatment in the absence or presence of 10^{-7} M leptin (n = 4–5). (d) Dose response effects of leptin on *Ptpn1* mRNA expression in WT mice (n = 5–6). All values are means ± SEM. Statistical analyses were performed by either unpaired *t*-test (a), two-way ANOVA (b, c) or one-way ANOVA (d). *, $p < 0.05$ versus control in WT. †, $p < 0.05$ versus leptin in WT. Ns; not significant.

3.9. STAT3 Phosphorylation Induced by Leptin Does Not Affect Hypothalamic Inflammation Induced by TNFα

Incubation with leptin induced STAT3 phosphorylation in the hypothalamic cultures (Fig. 7a). On the other hand, leptin treatment did not affect the mRNA expression levels of *Tnf*, *Il10* or *Il1b* after TNFα treatment (Fig. 7b, c and Supplementary Fig. 6). Incubation with 10^{-6} M but not 10^{-7} M or 10^{-8} M leptin significantly increased the *Ptpn1* mRNA expression levels in hypothalamic cultures (Fig. 7d).

4. Discussion

In the present study, we demonstrated that hypothalamic inflammation induced by a HFD, as assessed by the expression levels of TNFα and IL-10, was significantly attenuated, and that STAT3 phosphorylation in microglia in the arcuate nucleus was more increased in PTP1B KO compared to WT mice. Using hypothalamic cultures, we showed that inflammation induced by TNFα was significantly attenuated, accompanied by increased phosphorylation of both JAK2 and STAT3, in KO compared to WT mice. In addition, incubation with inhibitors of STAT3 phosphorylation or microglial depletion eliminated the difference in inflammation between the genotypes. Furthermore, we found that injection of leptin increased STAT3 phosphorylation in hypothalamic neurons and astrocytes and significantly increased STAT3 phosphorylation in hypothalamic cultures, but it did not affect inflammation. Thus, our data suggest that the deficiency of PTP1B attenuated hypothalamic inflammation via the activation of the JAK2-STAT3 signaling pathway in microglial cells.

It is reported that a HFD reduces leptin-induced STAT3 phosphorylation in the arcuate nucleus of WT mice (Munzberg et al., 2004), and that leptin sensitivity in hypothalamic neurons was increased in PTP1B KO compared to WT mice, which makes KO mice resistant to diet-induced obesity (Zabolotny et al., 2002; Bence et al., 2006). In the present study, hypothalamic inflammation, which could be related to obesity and leptin resistance (De Git and Adan, 2015), was examined in mice at the age of 7 weeks when there were no significant differences in body weight between the WT and KO mice fed a HFD. Thus, the comparison between genotypes in the present study has provided us with an opportunity to elucidate the underlying mechanisms by which body weight is increased in WT compared to KO mice on a HFD.

Consistent with previous studies (De Souza et al., 2005; Valdearcos et al., 2014), our data showed that TNFα immunoreactivity was increased in the arcuate nucleus in WT mice maintained on a HFD, but this was not the case in PTP1B KO mice. The analyses of *Tnf* and *Il10* mRNA expression levels further support the conclusion that inflammation in the hypothalamus was not activated in KO mice at the age of 7 weeks. Thus, it is indicated that hypothalamic inflammation preceded the relative increases in body weight in WT compared to KO mice fed a HFD. On the other hand, our data also showed that there were no significant differences in the activation of signaling pathways such as p65, p38, JNK and ERK between genotypes. This is probably because these signal transducers downstream from the TNFα receptor are not substrates for PTP1B (Tsou and Bence, 2012).

There are several lines of evidence that the JAK2-STAT3 signaling pathway functions downstream from the TNFα receptor (Romanatto et al., 2007; Guo et al., 1998; Miscia et al., 2002; Sica and Mantovani, 2012). The activated STAT3 is reported to constitute a dimer that translocates into the nucleus to exert anti-inflammatory effects by decreasing *Tnf* mRNA expression and increasing *Il10* mRNA expression (Benkhart et al., 2000; Hutchins et al., 2012, 2013). Conversely, STAT3 deficiency in macrophages is reported to increase inflammation (Takeda et al., 1999; Yoo et al., 2002), and previous studies revealed that PTP1B deficiency in macrophages decreased TNFα expression and increased IL-10 expression via activation of the STAT3 pathway in the peripheral tissues (Zhang et al., 2013; Grant et al., 2014; Pike et al., 2014). In the present study, we confirmed the findings of previous studies that STAT3 phosphorylation in the hypothalamus was increased in WT mice on a HFD (Ottaway et al., 2015; Knight et al., 2010; Martin et al., 2006). Our data also demonstrated that STAT3 phosphorylation in microglia increases more in KO mice than in WT mice on a HFD. The increased STAT3 phosphorylation is accompanied by the attenuation of hypothalamic inflammation *in vivo* and in primary hypothalamic cultures, and the inhibition of STAT3 phosphorylation as well as depletion of microglia completely eliminated the differences between genotypes in the cultures. These data suggest that PTP1B–deficiency in microglia activates the JAK2-STAT3 signaling pathways that lead to the attenuation of hypothalamic inflammation. Our data thus revealed an important role of the JAK2-STAT3 signaling pathway in hypothalamic microglia, a pathway that prevents hypothalamic inflammation and possibly obesity by a HFD. On the other hand, our data also showed that in WT mice, in which STAT3 phosphorylation is relatively low compared to KO mice, the decreased STAT3 phosphorylation by STAT3 inhibitors did not affect the inflammatory responses to the TNFα treatment (Fig.5 c-h), suggesting that the anti-inflammatory action of the JAK2-STAT3 pathway manifests only after the phosphorylation reaches certain levels.

In the present study, *in vivo* leptin treatment induced the phosphorylation of STAT3 in neurons and astrocytes but not in microglia, whereas it did not affect inflammation induced by TNFα in hypothalamic cultures (Pan et al., 2008; Wang et al., 2015). Consistent with our findings, it is demonstrated that leptin receptors are not expressed in microglia in mice (Pan et al., 2008). On the other hand, there are also reports showing that leptin phosphorylated STAT3 in microglial cells in rats or the BV-2 cell line (Tang et al., 2007; Pinteaux et al., 2007). While further studies are required to explain the discrepancies among studies, our data clearly indicate that the JAK2-STAT3 pathways have different roles among neurons and microglia: in the former, they mediate leptin signaling and in the latter they mediate signaling of cytokines such as

Please cite this article as: Tsunekawa, T., et al., Deficiency of PTP1B Attenuates Hypothalamic Inflammation via Activation of the JAK2-STAT3 Pathway in Microglia, EBioMedicine (2017), http://dx.doi.org/10.1016/j.ebiom.2017.01.007

TNFα. The graphical abstract shows schematic illustrations of the roles of the JAK2-STAT3 pathways in neurons and microglia, and in both, PTP1B negatively regulates the pathways.

Our data showed that TNFα and leptin treatment in hypothalamic cultures increased *Ptpn1* mRNA expression. The increased PTP1B could potentially decrease STAT3 phosphorylation and therefore activate inflammation in microglia, although the increases in *Ptpn1* expression were relatively small in the present study.

As TNFα transduces inflammatory signals in various tissues, including the hypothalamus (Purkayastha et al., 2011; De Git and Adan, 2015), it is plausible that TNFα in the hypothalamus induced by a HFD mediates the inflammation, at least partially. We therefore employed TNFα treatment and several inflammatory cytokines were indeed induced by the treatment in the present study. However, it is also possible that other inflammatory cytokines such as IL-1β and IL-6 are also induced by a HFD (Thaler et al., 2012; De Souza et al., 2005) and act on hypothalamic microglia to induce inflammation. Furthermore, other molecules downstream from the TNFα receptor that were not examined in this study might also play a role in hypothalamic inflammation. Our data also showed that STAT3 phosphorylation was increased not only in microglia but also in astrocytes in KO mice fed a HFD. Given that not only microglia but also astrocytes and neurons reportedly release inflammatory cytokines (Gupta et al., 2012; Wellhauser and Belsham, 2014), it is likely that there are some communications among these cells, and further studies are necessary to clarify the roles of microglia, astrocytes and neurons in hypothalamic inflammation.

In conclusion, we demonstrated that a deficiency of PTP1B attenuated hypothalamic inflammation via the activation of JAK2-STAT3 signaling pathway in microglial cells in mice under HFD conditions.

Funding Sources

This work was supported in part by a Grant-in Aid for Scientific Research (C) from the Japanese Society for Promotion of Science, Japan (23591302).

Conflicts of Interest

Not applicable.

Acknowledgements

We thank Michiko Yamada for helpful technical assistance.

Appendix A. Supplementary data

Supplementary data to this article can be found online at http://dx.doi.org/10.1016/j.ebiom.2017.01.007.

References

Adachi, K., Goto, M., Onoue, T., Tsunekawa, T., Shibata, M., Hagimoto, S., Ito, Y., Banno, R., Suga, H., Sugimura, Y., Oiso, Y., Arima, H., 2014. Mitogen-activated protein kinase phosphatase 1 negatively regulates MAPK signaling in mouse hypothalamus. Neurosci. Lett. 569, 49–54.

Argente-Arizon, P., Freire-Regatillo, A., Argente, J., Chowen, J.A., 2015. Role of non-neuronal cells in body weight and appetite control. Front. Endocrinol. (Lausanne) 6, 42.

Banno, R., Zimmer, D., De Jonghe, B.C., Atienza, M., Rak, K., Yang, W., Bence, K.K., 2010. PTP1B and SHP2 in POMC neurons reciprocally regulate energy balance in mice. J. Clin. Invest. 120, 720–734.

Bence, K.K., Delibegovic, M., Xue, B., Gorgun, C.Z., Hotamisligil, G.S., Neel, B.G., Kahn, B.B., 2006. Neuronal PTP1B regulates body weight, adiposity and leptin action. Nat. Med. 12, 917–924.

Benkhart, E.M., Siedlar, M., Wedel, A., Werner, T., Ziegler-Heitbrock, H.W., 2000. Role of Stat3 in lipopolysaccharide-induced IL-10 gene expression. J. Immunol. 165, 1612–1617.

Cheng, A., Uetani, N., Simoncic, P.D., Chaubey, V.P., Lee-Loy, A., Mcglade, C.J., Kennedy, B.P., Tremblay, M.L., 2002. Attenuation of leptin action and regulation of obesity by protein tyrosine phosphatase 1B. Dev. Cell 2, 497–503.

De Git, K.C., Adan, R.A., 2015. Leptin resistance in diet-induced obesity: the role of hypothalamic inflammation. Obes. Rev. 16, 207–224.

De Souza, C.T., Araujo, E.P., Bordin, S., Ashimine, R., Zollner, R.L., Boschero, A.C., Saad, M.J., Velloso, L.A., 2005. Consumption of a fat-rich diet activates a proinflammatory response and induces insulin resistance in the hypothalamus. Endocrinology 146, 4192–4199.

Dodd, G.T., Decherf, S., Loh, K., Simonds, S.E., Wiede, F., Balland, E., Merry, T.L., Munzberg, H., Zhang, Z.Y., Kahn, B.B., Neel, B.G., Bence, K.K., Andrews, Z.B., Cowley, M.A., Tiganis, T., 2015. Leptin and insulin act on POMC neurons to promote the browning of white fat. Cell 160, 88–104.

Friedman, J.M., 2009. Obesity: Causes and control of excess body fat. Nature 459, 340–342.

Grant, L., Shearer, K.D., Czopek, A., Lees, E.K., Owen, C., Agouni, A., Workman, J., Martin-Granados, C., Forrester, J.V., Wilson, H.M., Mody, N., Delibegovic, M., 2014. Myeloid-cell protein tyrosine phosphatase-1B deficiency in mice protects against high-fat diet and lipopolysaccharide-induced inflammation, hyperinsulinemia, and endotoxemia through an IL-10 STAT3-dependent mechanism. Diabetes 63, 456–470.

Guo, D., Dunbar, J.D., Yang, C.H., Pfeffer, L.M., Donner, D.B., 1998. Induction of Jak/STAT signaling by activation of the type 1 TNF receptor. J. Immunol. 160, 2742–2750.

Gupta, S., Knight, A.G., Gupta, S., Keller, J.N., Bruce-Keller, A.J., 2012. Saturated long-chain fatty acids activate inflammatory signaling in astrocytes. J. Neurochem. 120, 1060–1071.

Hagiwara, D., Arima, H., Morishita, Y., Wenjun, L., Azuma, Y., Ito, Y., Suga, H., Goto, M., Banno, R., Sugimura, Y., Shiota, A., Asai, N., Takahashi, M., Oiso, Y., 2014. Arginine vasopressin neuronal loss results from autophagy-associated cell death in a mouse model for familial neurohypophysial diabetes insipidus. Cell Death Dis. 5, e1148.

Hutchins, A.P., Poulain, S., Miranda-Saavedra, D., 2012. Genome-wide analysis of STAT3 binding in vivo predicts effectors of the anti-inflammatory response in macrophages. Blood 119, e110–e119.

Hutchins, A.P., Diez, D., Miranda-Saavedra, D., 2013. The IL-10/STAT3-mediated anti-inflammatory response: recent developments and future challenges. Brief. Funct. Genomics 12, 489–498.

Ito, Y., Banno, R., Hagimoto, S., Ozawa, Y., Arima, H., Oiso, Y., 2012. TNFalpha increases hypothalamic PTP1B activity via the NFkappaB pathway in rat hypothalamic organotypic cultures. Regul. Pept. 174, 58–64.

Ito, Y., Banno, R., Shibata, M., Adachi, K., Hagimoto, S., Hagiwara, D., Ozawa, Y., Goto, M., Suga, H., Sugimura, Y., Bettler, B., Oiso, Y., Arima, H., 2013. GABA type B receptor signaling in proopiomelanocortin neurons protects against obesity, insulin resistance, and hypothalamic inflammation in male mice on a high-fat diet. J. Neurosci. 33, 17166–17173.

Klaman, L.D., Boss, O., Peroni, O.D., Kim, J.K., Martino, J.L., Zabolotny, J.M., Moghal, N., Lubkin, M., Kim, Y.B., Sharpe, A.H., Stricker-Krongrad, A., Shulman, G.I., Neel, B.G., Kahn, B.B., 2000. Increased energy expenditure, decreased adiposity, and tissue-specific insulin sensitivity in protein-tyrosine phosphatase 1B-deficient mice. Mol. Cell. Biol. 20, 5479–5489.

Knight, Z.A., Hannan, K.S., Greenberg, M.L., Friedman, J.M., 2010. Hyperleptinemia is required for the development of leptin resistance. PLoS One 5, e11376.

Martin, T.L., Alquier, T., Asakura, K., Furukawa, N., Preitner, F., Kahn, B.B., 2006. Diet-induced obesity alters AMP kinase activity in hypothalamus and skeletal muscle. J. Biol. Chem. 281, 18933–18941.

Minokoshi, Y., Alquier, T., Furukawa, N., Kim, Y.B., Lee, A., Xue, B., Mu, J., Foufelle, F., Ferre, P., Birnbaum, M.J., Stuck, B.J., Kahn, B.B., 2004. AMP-kinase regulates food intake by responding to hormonal and nutrient signals in the hypothalamus. Nature 428, 569–574.

Miscia, S., Marchisio, M., Grilli, A., Di Valerio, V., Centurione, L., Sabatino, G., Garaci, F., Zauli, G., Bonvini, E., Di Baldassarre, A., 2002. Tumor necrosis factor alpha (TNF-alpha) activates Jak1/Stat3-Stat5B signaling through TNFR-1 in human B cells. Cell Growth Differ. 13, 13–18.

Morton, G.J., Cummings, D.E., Baskin, D.G., Barsh, G.S., Schwartz, M.W., 2006. Central nervous system control of food intake and body weight. Nature 443, 289–295.

Munzberg, H., Flier, J.S., Bjorbaek, C., 2004. Region-specific leptin resistance within the hypothalamus of diet-induced obese mice. Endocrinology 145, 4880–4889.

Myers, M.P., Andersen, J.N., Cheng, A., Tremblay, M.L., Horvath, C.M., Parisien, J.P., Salmeen, A., Barford, D., Tonks, N.K., 2001. TYK2 and JAK2 are substrates of protein-tyrosine phosphatase 1B. J. Biol. Chem. 276, 47771–47774.

Onoue, T., Goto, M., Tominaga, T., Sugiyama, M., Tsunekawa, T., Hagiwara, D., Banno, R., Suga, H., Sugimura, Y., Arima, H., 2016. Reactive oxygen species mediate insulin signal transduction in mouse hypothalamus. Neurosci. Lett. 619, 1–7.

Ottaway, N., Mahbod, P., Rivero, B., Norman, L.A., Gertler, A., D'alessio, D.A., Perez-Tilve, D., 2015. Diet-induced obese mice retain endogenous leptin action. Cell Metab. 21, 877–882.

Pan, W., Hsuchou, H., He, Y., Sakharkar, A., Cain, C., Yu, C., Kastin, A.J., 2008. Astrocyte leptin receptor (ObR) and leptin transport in adult-onset obese mice. Endocrinology 149, 2798–2806.

Paxinos, G., Franklin, K.J., 2000. The Mouse Brain in Stereotaxic Coordinates. Academic Press, New York.

Picardi, P.K., Calegari, V.C., Prada, P.O., Moraes, J.C., Araujo, E., Marcondes, M.C., Ueno, M., Carvalheira, J.B., Velloso, L.A., Saad, M.J., 2008. Reduction of hypothalamic protein tyrosine phosphatase improves insulin and leptin resistance in diet-induced obese rats. Endocrinology 149, 3870–3880.

Pike, K.A., Hutchins, A.P., Vinette, V., Theberge, J.F., Sabbagh, L., Tremblay, M.L., Miranda-Saavedra, D., 2014. Protein tyrosine phosphatase 1B is a regulator of the interleukin-10-induced transcriptional program in macrophages. Sci. Signal. 7, ra43.

Pinteaux, E., Inoue, W., Schmidt, L., Molina-Holgado, F., Rothwell, N.J., Luheshi, G.N., 2007. Leptin induces interleukin-1beta release from rat microglial cells through a caspase 1 independent mechanism. J. Neurochem. 102, 826–833.

Purkayastha, S., Zhang, G., Cai, D., 2011. Uncoupling the mechanisms of obesity and hypertension by targeting hypothalamic IKK-beta and NF-kappaB. Nat. Med. 17, 883–887.

Romanatto, T., Cesquini, M., Amaral, M.E., Roman, E.A., Moraes, J.C., Torsoni, M.A., Cruz-Neto, A.P., Velloso, L.A., 2007. TNF-alpha acts in the hypothalamus inhibiting food intake and increasing the respiratory quotient–effects on leptin and insulin signaling pathways. Peptides 28, 1050–1058.

Sato, I., Arima, H., Ozaki, N., Watanabe, M., Goto, M., Hayashi, M., Banno, R., Nagasaki, H., Oiso, Y., 2005. Insulin inhibits neuropeptide Y gene expression in the arcuate nucleus through GABAergic systems. J. Neurosci. 25, 8657–8664.

Shibata, M., Banno, R., Sugiyama, M., Tominaga, T., Onoue, T., Tsunekawa, T., Azuma, Y., Hagiwara, D., Lu, W., Ito, Y., Goto, M., Suga, H., Sugimura, Y., Oiso, Y., Arima, H., 2016. AgRP neuron-specific deletion of glucocorticoid receptor leads to increased energy expenditure and decreased body weight in female mice on a high-fat diet. Endocrinology 157, 1457–1466.

Sica, A., Mantovani, A., 2012. Macrophage plasticity and polarization: in vivo veritas. J. Clin. Invest. 122, 787–795.

Song, G.J., Jung, M., Kim, J.H., Park, H., Rahman, M.H., Zhang, S., Zhang, Z.Y., Park, D.H., Kook, H., Lee, I.K., Suk, K., 2016. A novel role for protein tyrosine phosphatase 1B as a positive regulator of neuroinflammation. J. Neuroinflammation 13, 86.

Stein, C.J., Colditz, G.A., 2004. The epidemic of obesity. J. Clin. Endocrinol. Metab. 89, 2522–2525.

Takeda, K., Clausen, B.E., Kaisho, T., Tsujimura, T., Terada, N., Forster, I., Akira, S., 1999. Enhanced Th1 activity and development of chronic enterocolitis in mice devoid of Stat3 in macrophages and neutrophils. Immunity 10, 39–49.

Tang, C.H., Lu, D.Y., Yang, R.S., Tsai, H.Y., Kao, M.C., Fu, W.M., Chen, Y.F., 2007. Leptin-induced IL-6 production is mediated by leptin receptor, insulin receptor substrate-1, phosphatidylinositol 3-kinase, Akt, NF-kappaB, and p300 pathway in microglia. J. Immunol. 179, 1292–1302.

Thaler, J.P., Yi, C.X., Schur, E.A., Guyenet, S.J., Hwang, B.H., Dietrich, M.O., Zhao, X., Sarruf, D.A., Izgur, V., Maravilla, K.R., Nguyen, H.T., Fischer, J.D., Matsen, M.E., Wisse, B.E., Morton, G.J., Horvath, T.L., Baskin, D.G., Tschop, M.H., Schwartz, M.W., 2012. Obesity is associated with hypothalamic injury in rodents and humans. J. Clin. Invest. 122, 153–162.

Tsou, R.C., Bence, K.K., 2012. Central regulation of metabolism by protein tyrosine phosphatases. Front. Neurosci. 6, 192.

Valdearcos, M., Robblee, M.M., Benjamin, D.I., Nomura, D.K., Xu, A.W., Koliwad, S.K., 2014. Microglia dictate the impact of saturated fat consumption on hypothalamic inflammation and neuronal function. Cell Rep. 9, 2124–2138.

Vinet, J., Weering, H.R., Heinrich, A., Kalin, R.E., Wegner, A., Brouwer, N., Heppner, F.L., Rooijen, N., Boddeke, H.W., Biber, K., 2012. Neuroprotective function for ramified microglia in hippocampal excitotoxicity. J. Neuroinflammation 9, 27.

Wang, Y., Hsuchou, H., He, Y., Kastin, A.J., Pan, W., 2015. Role of Astrocytes in Leptin Signaling. J. Mol. Neurosci. 56, 829–839.

Wellhauser, L., Belsham, D.D., 2014. Activation of the omega-3 fatty acid receptor GPR120 mediates anti-inflammatory actions in immortalized hypothalamic neurons. J. Neuroinflammation 11, 60.

White, C.L., Whittington, A., Barnes, M.J., Wang, Z., Bray, G.A., Morrison, C.D., 2009. HF diets increase hypothalamic PTP1B and induce leptin resistance through both leptin-dependent and -independent mechanisms. Am. J. Physiol. Endocrinol. Metab. 296, E291–E299.

Yoo, J.Y., Huso, D.L., Nathans, D., Desiderio, S., 2002. Specific ablation of Stat3beta distorts the pattern of Stat3-responsive gene expression and impairs recovery from endotoxic shock. Cell 108, 331–344.

Zabolotny, J.M., Bence-Hanulec, K.K., Stricker-Krongrad, A., Haj, F., Wang, Y., Minokoshi, Y., Kim, Y.B., Elmquist, J.K., Tartaglia, L.A., Kahn, B.B., Neel, B.G., 2002. PTP1B regulates leptin signal transduction in vivo. Dev. Cell 2, 489–495.

Zabolotny, J.M., Kim, Y.B., Welsh, L.A., Kershaw, E.E., Neel, B.G., Kahn, B.B., 2008. Protein-tyrosine phosphatase 1B expression is induced by inflammation in vivo. J. Biol. Chem. 283, 14230–14241.

Zhang, X., Zhang, G., Zhang, H., Karin, M., Bai, H., Cai, D., 2008. Hypothalamic IKKbeta/NF-kappaB and ER stress link overnutrition to energy imbalance and obesity. Cell 135, 61–73.

Zhang, J., Wang, B., Zhang, W., Wei, Y., Bian, Z., Zhang, C.Y., Li, L., Zen, K., 2013. Protein tyrosine phosphatase 1B deficiency ameliorates murine experimental colitis via the expansion of myeloid-derived suppressor cells. PLoS One 8, e70828.

Zhang, Z.Y., Dodd, G.T., Tiganis, T., 2015. Protein tyrosine phosphatases in hypothalamic insulin and leptin signaling. Trends Pharmacol. Sci. 36, 661–674.

Please cite this article as: Tsunekawa, T., et al., Deficiency of PTP1B Attenuates Hypothalamic Inflammation via Activation of the JAK2-STAT3 Pathway in Microglia, EBioMedicine (2017), http://dx.doi.org/10.1016/j.ebiom.2017.01.007

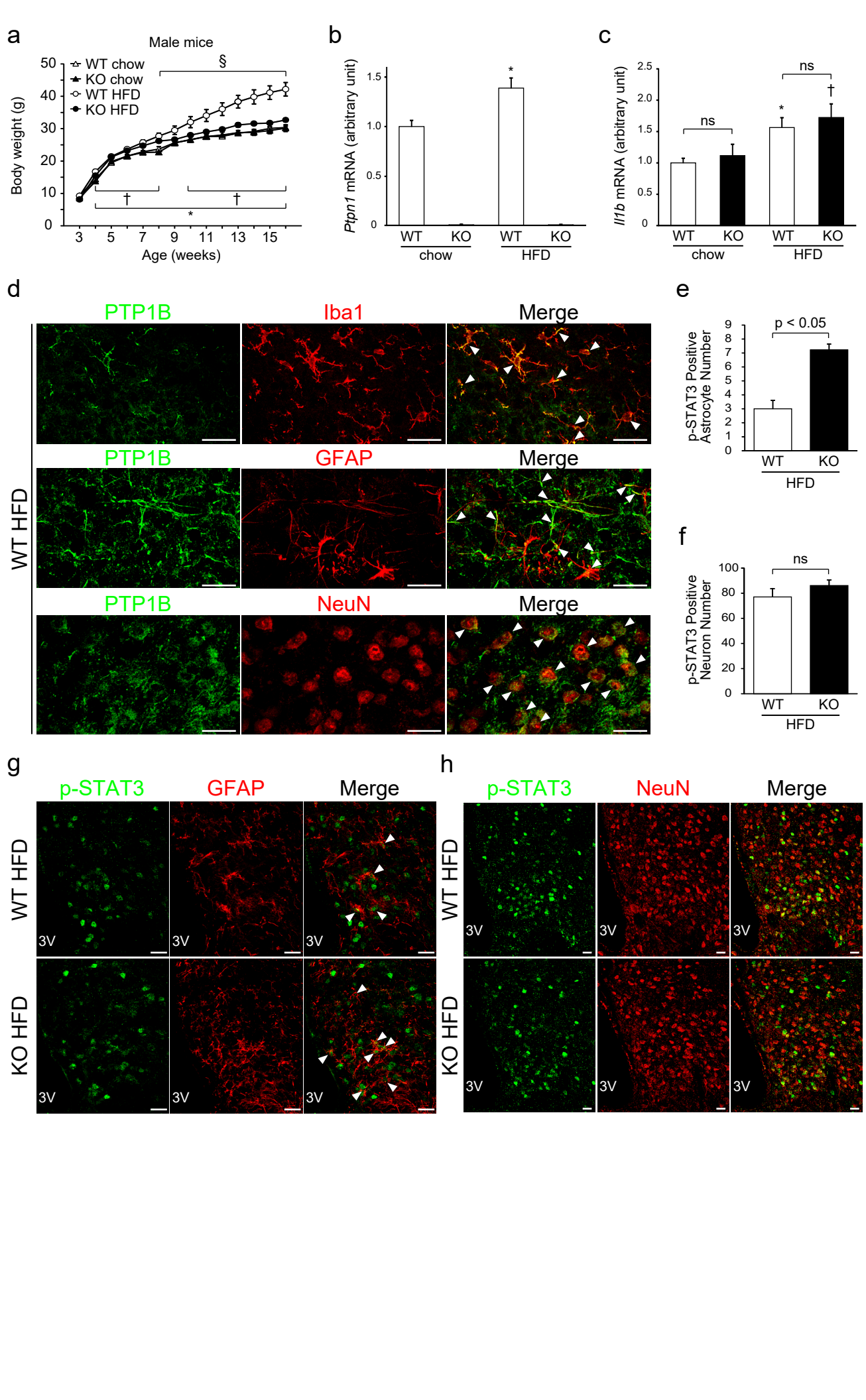
a
Male mice
WT chow
KO chow
WT HFD
KO HFD
Body weight (g)
Age (weeks)
§
†
†
*
b
Ptpn1 mRNA (arbitrary unit)
WT
KO
WT
KO
chow
HFD
c
Il1b mRNA (arbitrary unit)
ns
ns
*
†
WT
KO
WT
KO
chow
HFD
d
PTP1B
Iba1
Merge
PTP1B
GFAP
Merge
PTP1B
NeuN
Merge
WT HFD
e
p-STAT3 Positive Astrocyte Number
p < 0.05
WT
KO
HFD
f
p-STAT3 Positive Neuron Number
ns
WT
KO
HFD
g
p-STAT3
GFAP
Merge
WT HFD
KO HFD
3V
h
p-STAT3
NeuN
Merge
WT HFD
KO HFD
3V

Supplementary Figure 1. Body weight changes, expression of PTP1B, IL-1β genes and phosphorylation of STAT3.

(a) Body weights of male $PTP1B^{+/+}$ (WT) and $PTP1B^{-/-}$ (KO) mice on a chow diet or a HFD (n = 6 for a chow diet; n = 11 for a HFD). (b and c) The mRNA expression levels of *Ptpn1* (b) and *Il1b* (c) in the arcuate nucleus of WT and KO male mice at the age of 7 weeks on a chow diet or a HFD (n = 7-9). (d) Immunostaining of PTP1B together with Iba1, GFAP or NeuN in the arcuate nucleus of WT male mice at the age of 7 weeks on a HFD. White arrow heads show colocalization of microglia, astrocyte or neuron with PTP1B. (e-h) Immunostaining of pSTAT3 with GFAP (g) or NeuN (h) in the arcuate nucleus of WT and KO male mice on a HFD at the age of 7 weeks. White arrow heads show colocalization of astrocytes with p-STAT3 (g). The p-STAT3-positive cell number in astrocytes (e) or neurons (f) in the arcuate nucleus (n = 6 for astrocytes; n = 4 for neurons). All values are means ± SEM. Statistical analyses were performed by either two-way ANOVA with repeated measures (a), unpaired *t*-test (b, e and f) or two-way ANOVA (c). *, $p < 0.05$ versus chow in WT. †, $p < 0.05$ versus chow in KO. §, $p < 0.05$ versus HFD in WT. Ns, not significant. Scale bar = 20 μm. 3V: third ventricle.

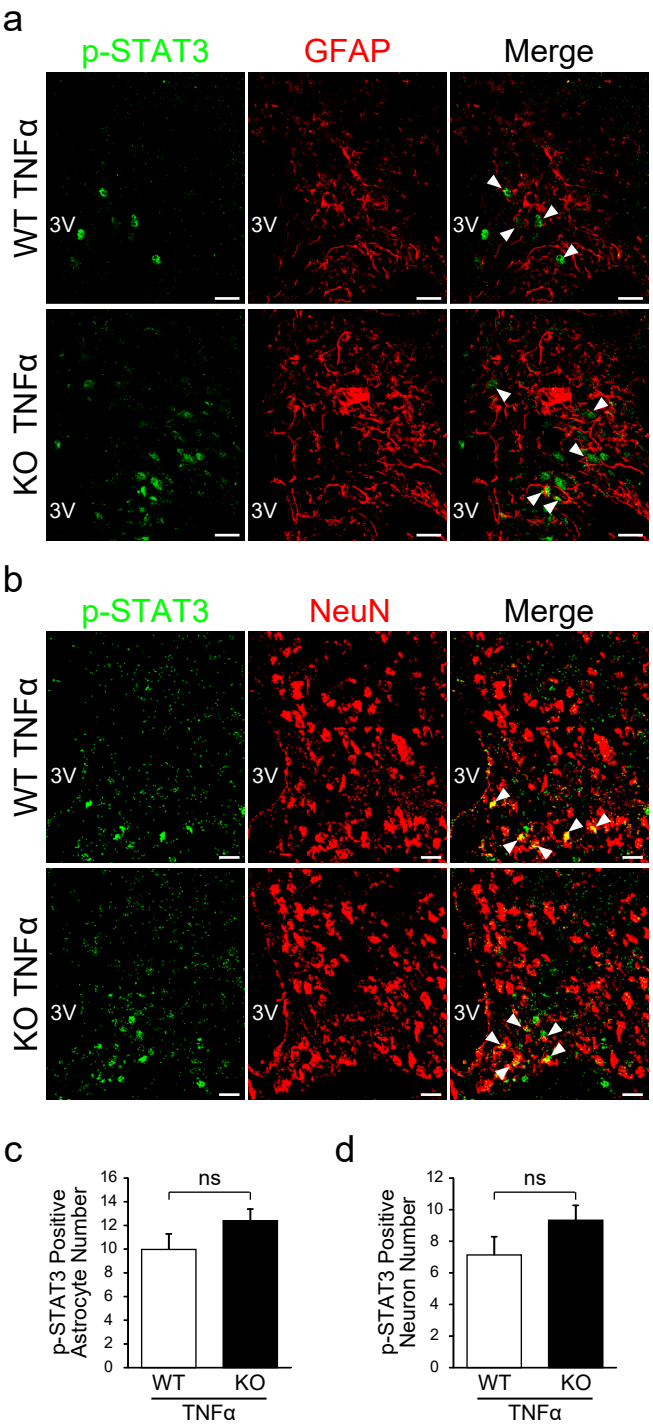

Supplementary Figure 2. Analysis of STAT3 phosphorylation in astrocytes and neurons in the hypothalamus after icv injection of TNFα.

Immunostaining of p-STAT3 together with GFAP (a) or NeuN (b) after icv injection of 10^{-12} M TNFα in the arcuate nucleus of male WT and KO mice at the age of 10 weeks on a chow diet after 12 h fasting. White arrow heads show colocalization of p-STAT3 with astrocytes (a) or neurons (b). The p-STAT3-positive cell number in astrocytes (c) or neurons (d) in the arcuate nucleus (n = 5). All values are means ± SEM. Statistical analyses were performed by unpaired *t*-test. Ns; not significant. Scale bar = 20 μm. 3V: third ventricle.

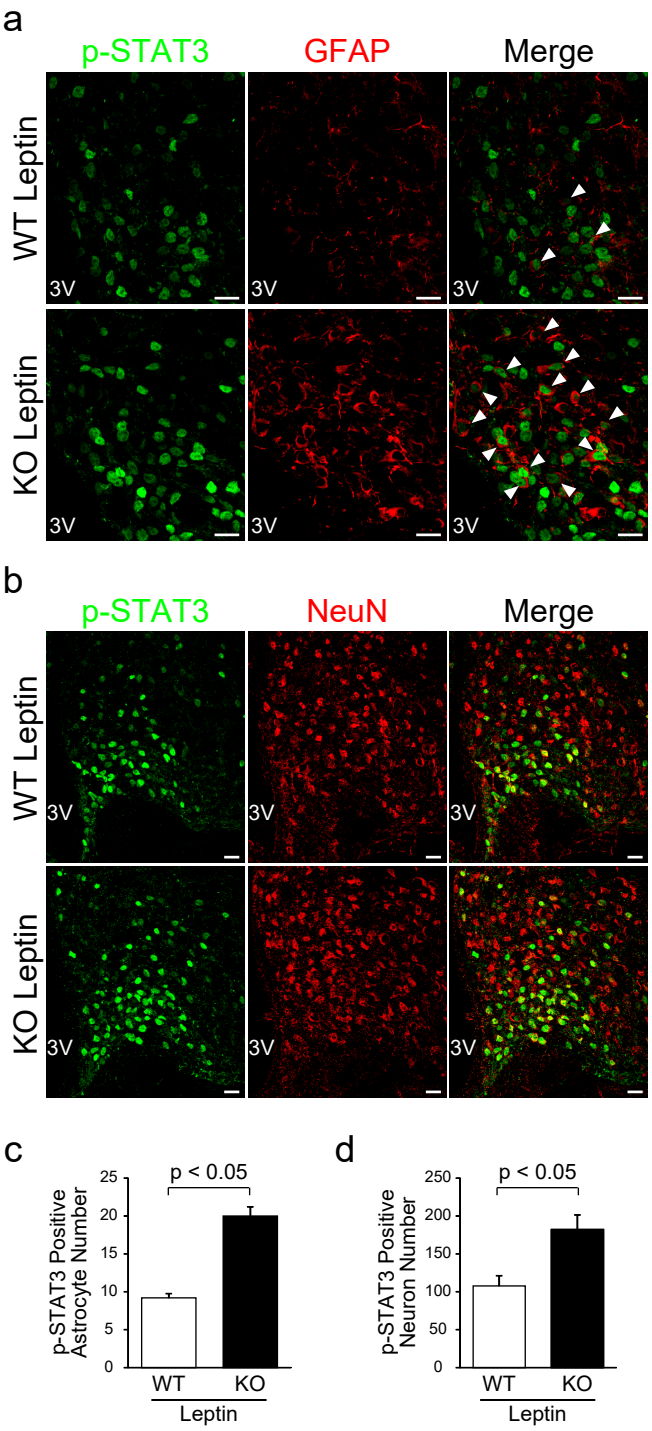

Supplementary Figure 3. Analysis of STAT3 phosphorylation in astrocytes and neurons in the hypothalamus after ip injection of leptin.

Immunostaining of p-STAT3 together with GFAP (a) or NeuN (b) in the arcuate nucleus after ip injection of 1 μg/g leptin in WT and KO male mice at the age of 10 weeks on a chow diet after 12 h fasting. White arrows show colocalization of astrocytes (a) with p-STAT3. The p-STAT3-positive cell numbers in astrocytes (c) or neurons (d) in the arcuate nucleus (n = 5 for astrocytes; n = 4 for neurons). All values are means ± SEM. Statistical analyses were performed by unpaired *t*-test. Scale bar = 20 μm. 3V: third ventricle.

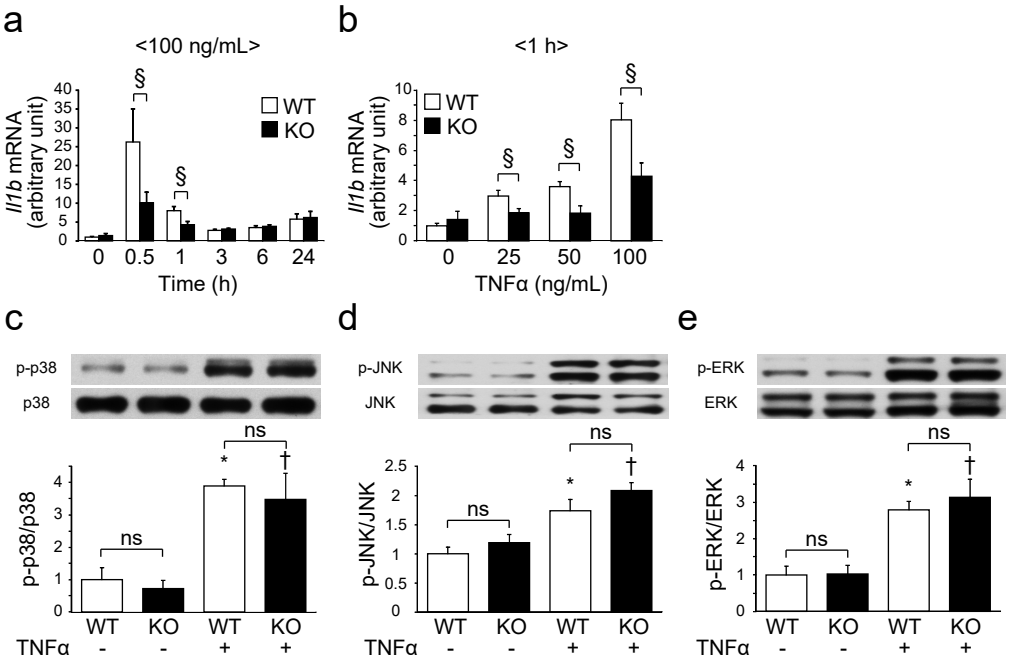

Supplementary Figure 4. Effects of TNFα on the mRNA expression levels of inflammatory cytokines and phosphorylation of p38, JNK and ERK in hypothalamic slice cultures.

Time-course (a) and dose response (b) effects of TNFα on the mRNA expression levels of *Il1β* in WT and KO mice (n = 4-5). The phosphorylation of p38 (c), JNK (d) and ERK (e) treated with 100 ng/mL TNFα (n = 4-5). All values are mean ± SEM. Statistical analyses were performed by two-way ANOVA. *, $p < 0.05$ versus control in WT. †, $p < 0.05$ versus control in KO. §, $p < 0.05$ versus TNFα in WT. Ns; not significant.

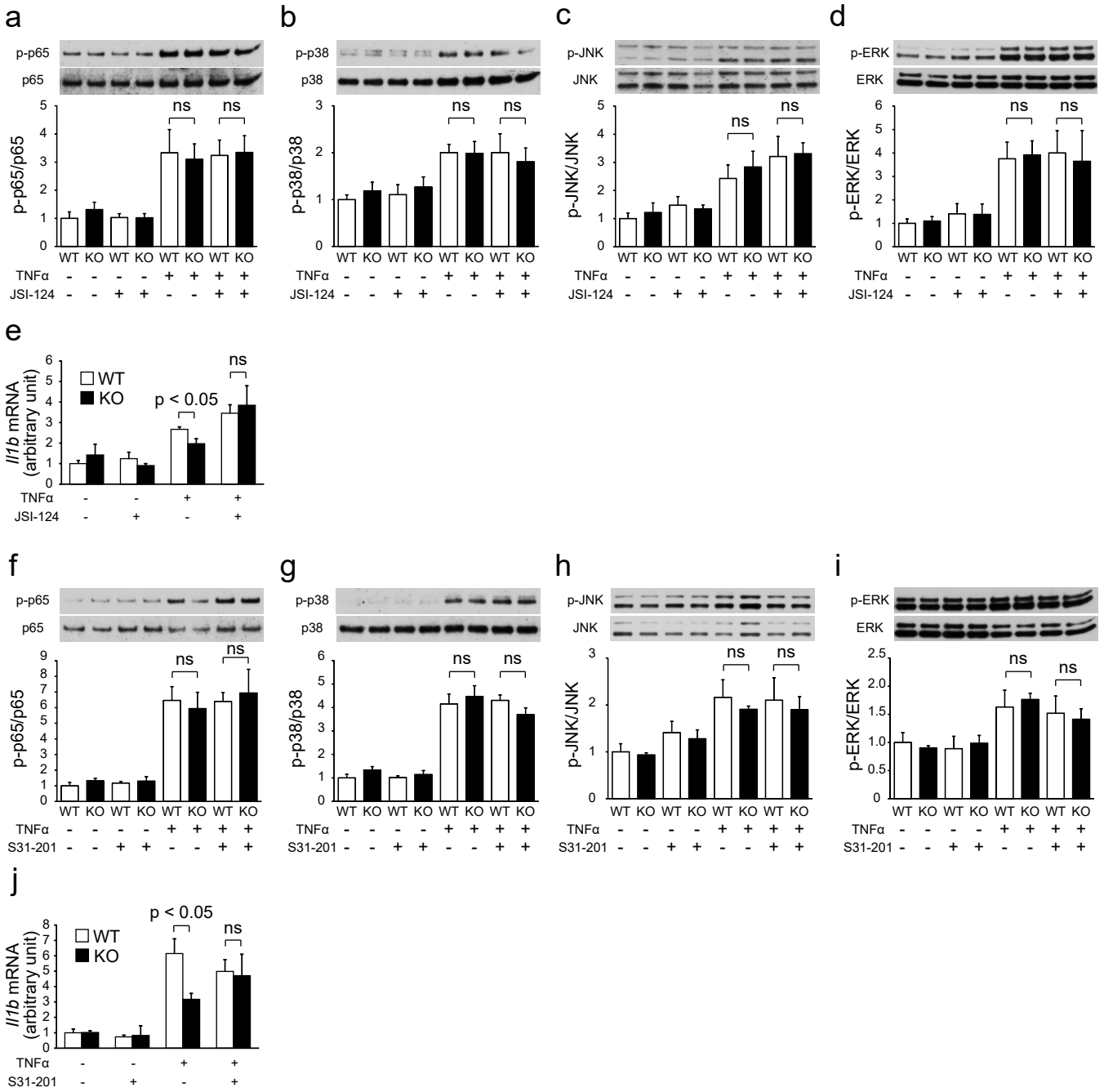

Supplementary Figure 5. Effects of blockade of the JAK2-STAT3 pathway on the phosphorylation of p65, p38, JNK and ERK, and the mRNA expression level of *Il1b* in hypothalamic slice cultures.

The phosphorylation of p65 (a and f), p38 (b and g), JNK (c and h) and ERK (d and i) induced by 100 ng/mL TNFα in the absence or presence of JSI-124 or S31-201 in WT and KO mice (n = 3-5). (e and j) The mRNA expression of *Il1b* induced by TNFα in the absence or presence of JSI-124 (e) or S31-201 (j) in WT and KO (n = 3-6). All values are means ± SEM. Statistical analyses were performed by two-way ANOVA. Ns; not significant.

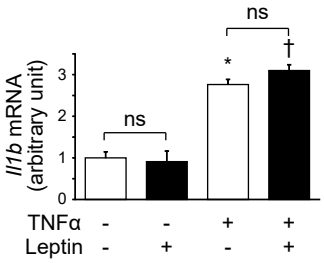

Supplementary Figure 6. Effects of leptin on the mRNA expression level of *Il1b* in the hypothalamus of WT mice.

The mRNA expression level of *Il1b* induced by 100 ng/mL TNFα in the absence or presence of 10^{-7} M leptin in hypothalamic slice explants of WT mice (n = 4-5). All values are means ± SEM. Statistical analyses were performed by two-way ANOVA. *, $p < 0.05$ versus control in WT. †, $p < 0.05$ versus leptin in WT. Ns; not significant.

Gene	Forward primer (5'→3')	Reverse primer (5'→3')
Tnf	CATCTTCTCAAAATTCGAGTGACAA	TGGGAGTAGACAAGGTACAACCC
Il10	GGTTGCCAAGCCTTATCGGA	ACCTGCTCCACTGCCTTGCT
Il1b	CGACAAAATACCTGTGGCCT	TTCTTTGGGTATTGCTTGGG
Il6	GTGGCTAAGGACCAAGACCA	GGTTTGCCGAGTAGACCTCA
Ptpn1	GCGCTTCTCCTACCTGGCTGTCAT	ACGTGCTCGGGTGGAAGGTCTA
Aif1	TGATCCCAAATACAGCAATGATGAG	TCCAGCATTCGCTTCAAGGAC
Cd68	CTTCCCACAAGCAGCACAG	AATGATGAGAGGCAGCAAGAGA
Adgre1	AATCGCTGCTGGTTGAATACAG	CCAGGCAAGGAGGACAGAGTT
Gfap	AACGACTATCGCCGCCAACTG	CTCTTCCTGTTCGCGCATTTG
Tubb3	CTGGAACCATGGACAGTGTTCG	CGACATCTAGGACTGAGTCCAC
Pomc	GAGGCCACTGAACATCTTTGTC	GCAGAGGCAAACAAGATTGG
Agrp	GCGGAGGTGCTAGATCCACA	AGGACTCGTGCAGCCTTACAC
Gapdh	AGGTCGGTGTGAACGGATTTG	TGTAGACCATGTAGTTGAGGTCA

Supplementary Table 1.

List of qRT-PCR primers used in this study.

	WT	KO
Iba1 cells / pSTAT3 positive cells (%)	10.22 ± 0.38	14.64 ± 0.83[§]
GFAP cells / pSTAT3 positive cells (%)	3.32 ± 0.19	7.96 ± 1.11[§]
NeuN cells / pSTAT3 positive cells (%)	78.65 ± 2.67	73.24 ± 1.43

Supplementary Table 2. The percentages of microglia, astrocytes and neurons constituting the pSTAT3-positive population in the arcuate nucleus on a HFD.

All values are means ± SEM (n = 6 for microglia and astrocytes; n = 4 for neurons). Statistical analyses were performed by unpaired *t*-test. §, $p < 0.05$ versus HFD in WT.

	WT	KO
Iba1 cells / pSTAT3 positive cells (%)	33.77 ± 1.37	43.77 ± 1.05[§]
GFAP cells / pSTAT3 positive cells (%)	30.59 ± 1.47	27.72 ± 2.61
NeuN cells / pSTAT3 positive cells (%)	40.69 ± 3.60	28.70 ± 3.54[§]

Supplementary Table 3. The percentages of microglia, astrocytes or neurons constituting the pSTAT3-positive population in the arcuate nucleus after icv injection of TNFα. All values are means ± SEM (n = 5). Statistical analyses were performed by unpaired *t*-test. §, $p < 0.05$ versus TNFα in WT.

	WT	KO
Iba1 cells / pSTAT3 positive cells (%)	0.37 ± 0.14	0.29 ± 0.06
GFAP cells / pSTAT3 positive cells (%)	7.42 ± 0.56	9.37 ± 0.85
NeuN cells / pSTAT3 positive cells (%)	83.70 ± 4.23	86.61 ± 4.88

Supplementary Table 4. The percentages of microglia, astrocytes or neurons constituting the pSTAT3-positive population in the arcuate nucleus after ip injection of leptin. All values are means ± SEM (n = 4 for microglia and neurons; n = 5 for astrocytes).